REPORT No. 352

LARGE-SCALE AERODYNAMIC CHARACTERISTICS OF AIRFOILS AS TESTED IN THE VARIABLE DENSITY WIND TUNNEL

By EASTMAN N. JACOBS and RAYMOND F. ANDERSON

Langley Memorial Aeronautical Laboratory

41630—31——2S

REPORT No. 352

LARGE-SCALE AERODYNAMIC CHARACTERISTICS OF AIRFOILS AS TESTED IN THE VARIABLE DENSITY WIND TUNNEL

By Eastman N. Jacobs and Raymond F. Anderson

SUMMARY

In order to give the large-scale characteristics of a variety of airfoils in a form which will be of maximum value, both for airplane design and for the study of airfoil characteristics, a collection has been made of the results of airfoil tests made at full-scale values of the Reynolds Number in the variable density wind tunnel of the National Advisory Committee for Aeronautics. They have been corrected for tunnel wall interference and are presented not only in the conventional form but also in a form which facilitates the comparison of airfoils and from which corrections may be easily made to any aspect ratio.

An example showing the method of correcting the results to a desired aspect ratio has been given for the convenience of designers. In addition, the data have been analyzed with a view to finding the variation of the aerodynamic characteristics of airfoils with their thickness and camber.

INTRODUCTION

The results of large-scale airfoil tests from the variable density wind tunnel are to be preferred for most practical purposes to those obtained at a comparatively low scale from atmospheric wind tunnels. The results of the large-scale tests not only approach more closely those obtained under full-scale conditions, as shown by comparison with flight tests (Reference 13), but are also more consistent among themselves. It is well known, for example, that an airfoil may show different aerodynamic characteristics as a result of low-scale tests in different wind tunnels. As the scale is increased, however, such discrepancies, resulting from differences in the turbulence of the air streams, become smaller, certain aerodynamic peculiarities disappear, and the relation of the aerodynamic characteristics to the profile shape becomes more consistent.

The large-scale aerodynamic characteristics of a considerable variety of airfoils have been available from tests made in the variable density wind tunnel during the period between the completion of the tunnel (April, 1923) and the destruction of its interior by fire (August, 1927). These large-scale characteristics, published in 10 different reports, were not given in a uniform manner and were uncorrected for tunnel-wall interference because the correction formulas had not yet been verified. Experimental verification of the theoretical wind-tunnel wall interference correction and a satisfactory method of correcting results from tests of rectangular airfoils to infinite aspect ratio have since led to the adoption of a standard form for the presentation of airfoil characteristics at the Langley Memorial Aeronautical Laboratory.

The object of this report is to collect all of the published large-scale results from tests on standard airfoil models in the variable density wind tunnel and to present them in a uniform manner so that the results of different tests may be easily compared. The new standard form has been used; that is, the airfoil characteristics are represented by two sets of curves. First, the characteristics corrected for tunnel wall effect to aspect ratio 6 in free air are plotted against the angle of attack. Second, the characteristics corresponding to a wing of infinite span are plotted against the lift coefficient. In this way the value of the data to the designer will be increased, because the airfoils may be more easily compared and because the characteristics of a given airfoil may be readily found for any desired aspect ratio. Moreover, by adopting a standard form of presentation, these results will now be conveniently available for future use in comparing them with the results from other wind tunnels and from the new variable density wind tunnel.

TESTS

A description of the tunnel and the method of making the tests is given in Reference 1. The airfoil models were all 5 by 30 inches and were made of duralumin, with the exception of the CYH, which was made of plaster of Paris. The tests given here were made at a pressure of 20 atmospheres and a Reynolds Number of 3,500,000, approximately. This value of the Reynolds Number represents the scale which would be obtained if a wing of 3.6-foot chord had been tested at 100 m. p. h. in air of normal density. The test conditions of the airfoils as given in References 2 to 11 were approximately the same except for the method of support. In the tests of References 2 and 3, which include the N. A. C. A. 97, 98, and 99, and the N. A. C. A.–M. series, the airfoils were supported by two

round wires extending vertically across the tunnel and by a sting projecting to the rear, which was also used to vary the angle of attack. The supports used in the tests of References 6 to 11, inclusive, were streamline struts extending from the balance platform to the lower surface and a sting similar to the one used previously. In the tests of Reference 5 the Göttingen 387 and the U. S. A. 35–B were supported by round wires and the U. S. A. 5, U. S. A. 27, U. S. A. 35–A, R. A. F. 15, and Clark Y by struts. The M–6 and M–12 curves (figs. 18, 19, 30, and 31) show the small difference in the results from the two methods of support. The Clark Y tests (figs. 74 and 75), in which strut supports were used, show the difference that may be produced by polishing the surface.

Method of correcting data.—The formulas used in correcting the data to infinite aspect ratio and for the influence of the tunnel walls are from the works of Munk, Glauert, and Prandtl, which are given in the N. A. C. A. reports, References 11 and 12. The notation and formulas used are as follows:

C_L = absolute lift coefficient.
D = diameter of wind-tunnel throat.
b = span of airfoil.
S = area of airfoil.
α = angle of attack in free air.
α_T = angle of attack as measured in the tunnel.
α_i = induced angle of attack.
α_o = angle of attack at which an airfoil of infinite span would give the same lift coefficient as the airfoil tested in the tunnel.
R = actual aspect ratio of airfoil.
R_e = effective aspect ratio of the airfoil; the aspect ratio of an airfoil which would give the same characteristics in free air as the airfoil tested in the tunnel.
C_{M_O} = moment coefficient about a point one-quarter of the chord behind the leading ledge.
C_D = absolute drag coefficient for an airfoil in free air.
C_{D_O} = profile drag coefficient.
C_{D_T} = absolute drag coefficient obtained from the tunnel tests.
C_{D_i} = induced drag coefficient.
τ = a factor correcting the induced angle of attack to allow for the change from elliptical span loading resulting from the use of an airfoil of rectangular plan form.
σ = a factor correcting the induced drag to allow for the change from elliptical span loading resulting from the use of an airfoil of rectangular plan form.
a = increase in lift coefficient per degree for an airfoil of aspect ratio R.
$a_o = \frac{dC_L}{d\alpha_o}$ = increase in lift coefficient per degree for an airfoil of infinite span.

The formulas for correcting the data from the closed throat tunnel conditions to free air are as follows:

$$\alpha = \alpha_T + \frac{C_L S}{2\pi D^2} \times 57.3.$$

(Angles of attack are measured in degrees.)

$$C_D = C_{D_T} + \frac{C_L^2 S}{2\pi D^2}.$$

Since the reduction to infinite aspect ratio was made from the uncorrected tunnel data, the effective aspect ratio (R_e) of the airfoil was used.

$$R_e = \frac{R}{1 - \frac{1}{2}\left(\frac{b}{D}\right)^2}$$

then

$$\alpha_o = \alpha_T - \frac{C_L}{\pi R_e}(1+\tau) \times 57.3$$

$$C_{D_o} = C_{D_T} - \frac{C_L^2}{\pi R_e}(1+\sigma).$$

RESULTS

The characteristics of the airfoils are presented by means of two independent sets of curves. The first is the conventional plot of C_L, C_D, L/D and $C.\ P.$ against angle of attack, but differs from most previous plots in that the results have been corrected for tunnel wall effects to aspect ratio 6. The second set of curves gives the deduced characteristics of an airfoil of infinite span. The profile drag coefficient C_{D_o}, the angle of attack α_o, and the moment coefficient about the quarter chord point C_{M_o}, are plotted against the lift coefficient. This type of plot, which has been used in England, has three important advantages over the more familiar type. First, the characteristics are plotted against the lift coefficient as abscissa because the lift coefficient is usually treated as the independent variable. Second, the efficiency and pitching characteristics of different airfoils may be compared very much more readily by comparing profile drag and moment coefficient curves rather than the familiar L/D and $C.\ P.$ curves. This is particularly true if the moment coefficient about a point one-quarter of the chord behind the leading edge is used, because its value for a given airfoil is approximately constant over the working range. Third, in applying the results of airfoil tests, it is almost always necessary to correct them to another aspect ratio, and it is more convenient to correct from an infinite than from some finite aspect ratio.

Correction to finite aspect ratio.—For convenience, the formulas for use in reducing these data to any aspect ratio will be summarized. If engineering coefficients are desired, the data should first be reduced to the desired aspect ratio in terms of the absolute coefficients by the use of the following formulas. The slope, and the lift and drag coefficients for a given

angle of attack should then be multiplied by 0.002558 to obtain the corresponding values of the engineering coefficients K_y and K_x.

The angle of attack in degrees for the lift coefficient C_L is:

$$\alpha=\alpha_0+\frac{C_L}{\pi R}(1+\tau)\times 57.3$$

or

$$\alpha=\alpha_0+\frac{18.24}{R}C_L(1+\tau).$$

The lift curve slope when angle of attack is measured in degrees is

$$a=\frac{a_0}{1+\frac{a_0}{\pi R}(1+\tau)\ 57.3.}$$

where a_0 is the slope for the wing of infinite span.

Assuming a mean value for a_0 of 0.0960 in the second term of the denominator, this becomes approximately:

$$a=\frac{a_0}{1+\frac{1.75}{R}(1+\tau).}$$

The value of a_0 for a wing of given thickness may be found from Figure 95.

The drag coefficient is

$$C_D=C_{D_0}+\frac{C_L^2}{\pi R}(1+\sigma).$$

The values of τ and σ depend on the shape of the span loading diagram of the airfoil. For an elliptical wing without effective twist they are zero and for a rectangular wing their values are given in Figure 1.

The moment coefficient at a given value of the lift coefficient may be taken as the same for any aspect ratio. The center of pressure, measured in per cent of chord from the leading edge, is given by

$$C.\ P.=25\text{ per cent}-\frac{C_{M_0}}{C_L\cos\alpha+C_D\sin\alpha}\cdot 100\text{ per cent.}$$

where C_{M_0} is the moment coefficient about a point one-quarter of the chord behind the leading edge. For most purposes the following approximations of the above formula give sufficient accuracy. The center of pressure measured as a fraction of the chord from the quarter-chord point is

$$C_p\left(\frac{c}{4}\right)=\frac{C_{M_0}}{C_L}.$$

or when measured from the leading edge in per cent of chord

$$C.\ P.=25\text{ per cent}-\frac{C_{M_0}}{C_L}\cdot 100\text{ per cent.}$$

The use of the foregoing formulas may be more easily understood from the following example. Suppose it is desired to find the aerodynamic characteristics of a rectangular Clark Y wing of aspect ratio 8. For a sample calculation a lift coefficient of 0.9 will be assumed.

The angle of attack for a given value of C_L is

$$\alpha=\alpha_0+\alpha_i$$
$$\alpha=\alpha_0+18.24\frac{C_L}{R}(1+\tau)$$

From Figure 1, for an aspect ratio of 8, $\tau=0.22$. Then

$$\alpha=\alpha_0+2.780\ C_L.$$

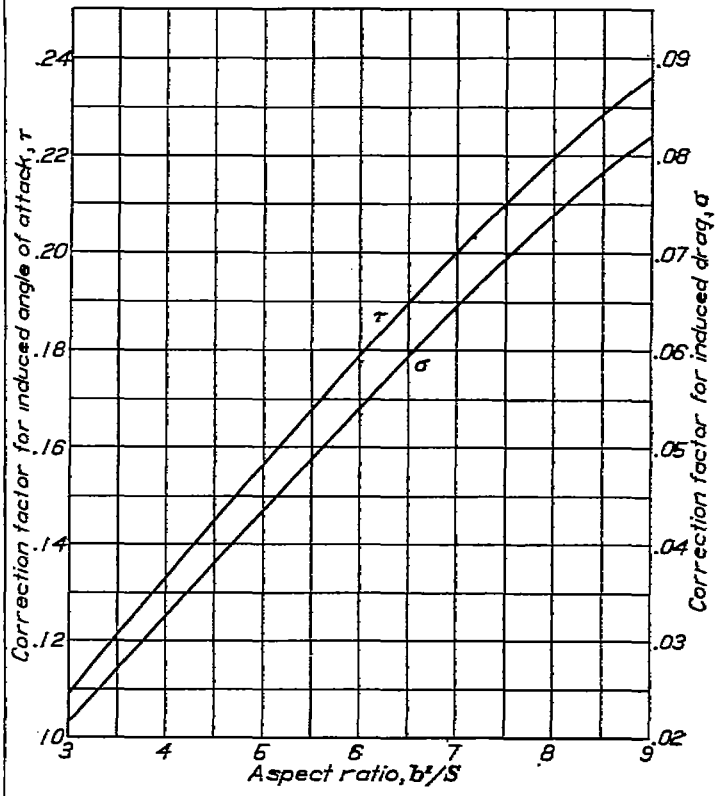

FIGURE 1.—Correction factors for rectangular airfoils. Based on $a_0=0.0960$

From Figure 75, when

$$C_L=0.9,\ \alpha_0=4.2°$$
$$\alpha=4.2+2.50$$
$$\alpha=6.7°.$$

The drag coefficient is

$$C_D=C_{D_0}+C_{D_i}$$
$$C_D=C_{D_0}+\frac{C_L^2}{\pi R}(1+\sigma).$$

From Figure 1, for an aspect ratio of 8, $\sigma=0.074$. Then

$$C_D=C_{D_0}+0.0427C_L^2.$$

From Figure 75, when $C_L = 0.9$, $C_{D_0} = 0.0145$

$$C_D = 0.0145 + 0.0346$$

$$C_D = 0.0491$$

$$\frac{L}{D} = \frac{0.9}{0.0491} = 18.3.$$

The moment coefficient about the quarter chord point, from Figure 75, is -0.07 for a lift coefficient of 0.9.

The center of pressure about the leading edge is

$$C.\ P._{\cdot} = 0.25 - \frac{C_{M_0}}{C_L}$$

$$C.\ P._{\cdot} = 0.25 + 0.0778$$

$C.\ P._{\cdot} = 32.8$ per cent of chord from the leading edge.

This will be the position of the center of pressure for an angle of attack of 6.7°. The calculations for other values of C_L may be conveniently tabulated in the following form. If the engineering coefficients (K_y and K_x) are desired, the values of columns 1, 5, 6, 7, and 9 should be multiplied by 0.002558.

1	2	3	4	5	6	7	8	9	10	11
C_L	α_0 degrees	$\frac{18.24}{\frac{C_L}{R}(1+\tau)}$	$\alpha_0+\alpha_t$	C_{p_0}	$\frac{C_L^2}{\pi R}(1+\sigma)$	$C_{D_0}+C_{D_i}$	$\frac{L}{D}$	C_{M_0}	$\frac{C_{M_0}}{C_L}$	$0.25-C.P.\left(\frac{c}{4}\right)$
		α_t	α degrees		C_{D_i}	C_D			C. P. $\left(\frac{c}{4}\right)$	Per cent C. P. (L. E.)
0	−5.1	0	−5.1	0.0108	0	0.0108	0	−0.082		
.20	−3.0	.6	−2.4	.0101	.0017	.0118	17.0	−.078	−.39	64
.40	−1.0	1.1	+0.1	.0101	.0068	.0169	23.7	−.074	−.18	43
.60	+1.1	1.7	2.8	.0111	.0154	.0265	22.6	−.074	−.12	37
.80	3.2	2.2	5.4	.0130	.0273	.0403	19.8	−.072	−.09	34
1.00	5.2	2.8	8.0	.0165	.0427	.0592	16.9	−.060	−.06	31
1.20	7.6	3.3	10.9	.0223	.0615	.0838	14.3	−.042	−.04	29
($C_{L\,max.}$)										
1.42	12.0	4.0	16.0	.0300	.0861	.1161	12.2	−.010	−.007	26
1.20	15.6	3.3	18.9		.0615			−.054	−.04	29

DISCUSSION

In the analysis of the data a study was made of the effect of profile shape upon the airfoil characteristics. Such an analysis is difficult not only because the effects of the large number of variables can not be separated, but also because there is no uniform variation of shape characteristics throughout the entire group of airfoils. A program involving the testing of a large family of airfoils in the new variable density wind tunnel has been formulated with a view to a more complete investigation of this subject. In spite of the limitations of the data available, it was found profitable to study the variation of aerodynamic characteristics with camber and thickness.

Certain characteristics need not be analyzed, either because they do not vary with thickness and camber, or because their variation may be predicted with reasonable accuracy by means of Munk's theory of airfoils. (Reference 12.) Within the working range below the burble region all of the airfoils, irrespective of their thickness and camber, exhibit an approximately constant value of the moment coefficient about the quarter chord point and approximately the same variation of the profile drag coefficient with the lift coefficient. The value of the moment coefficient and the angle of zero lift depend, as indicated by the theory, on the shape of the mean camber line. There remains to be analyzed, therefore, the maximum lift coefficient, the minimum profile drag coefficient, and the slope of the lift curve.

The effect of profile shape on these aerodynamic characteristics was studied by plotting them against maximum thickness and maximum mean camber. The maximum mean camber is the maximum displacement of the mean camber line of the airfoil section from the line connecting the leading and trailing edges. These plots, Figures 92 to 96, indicate certain general trends, but in studying them it should be remembered that the thickness and camber vary together and that the camber lines of the different airfoils are of very different shapes; the M series, for instance, are reflexed near the trailing edge to give approximately a stationary center of pressure. The trends may be summarized as follows:

1. The minimum profile drag increases as the maximum thickness and maximum mean camber are increased.

2. The maximum lift increases with thickness up to a thickness of 12 per cent of the chord beyond which it decreases.

3. The slope of the lift curve decreases as the maximum thickness is increased.

4. The ratio of maximum lift to minimum profile drag tends to decrease as the maximum thickness is increased, the tendency becoming very marked when the thickness is increased beyond 12 per cent.

LANGLEY MEMORIAL AERONAUTICAL LABORATORY,
NATIONAL ADVISORY COMMITTEE FOR AERONAUTICS,
LANGLEY FIELD, VA., *October 21, 1929.*

REFERENCES

1. Munk, Max M., and Miller, Elton W.: The Variable Density Wind Tunnel of the National Advisory Committee for Aeronautics. N. A. C. A. Technical Report No. 227, 1926.
2. Munk, Max M.: Preliminary Wing Model Tests in the Variable Density Wind Tunnel of the National Advisory Committee for Aeronautics. N. A. C. A. Technical Report No. 217, 1925.
3. Munk, Max M., and Miller, Elton W.: Model Tests with a Systematic Series of 27 Wing Sections at Full Reynolds Number. N. A. C. A. Technical Report No. 221, 1925.
4. Higgins, George J.: The Comparison of Well-Known and New Wing Sections Tested in the Variable Density Wind Tunnel. N. A. C. A. Technical Note No. 219, 1925.
5. Munk, Max M., and Miller, Elton W.: The Aerodynamic Characteristics of Seven Frequently Used Wing Sections at Full Reynolds Number. N. A. C. A. Technical Report No. 233, 1926.
6. Higgins, George J.: The N. A. C. A. CYH Airfoil Section. N. A. C. A. Technical Note No. 240, 1926.
7. ———: The Characteristics of the N. A. C. A.–M12 Airfoil Section. N. A. C. A. Technical Note No. 243, 1926.
8. Jacobs, Eastman N.: Characteristics of Propeller Sections Tested in the Variable Density Wind Tunnel. N. A. C. A. Technical Report No. 259, 1927.
9. Higgins, George J.: The Characteristics of the N. A. C. A. 97, Clark Y, and N. A. C. A.–M6 Airfoils with Particular Reference to the Angle of Attack. N. A. C. A. Technical Note No. 270, 1927.
10. ———: Wall Interference in Closed Type Wind Tunnels. N. A. C. A. Technical Note No. 256, 1927.
11. ———: The Effect of Walls in Closed Type Wind Tunnels. N. A. C. A. Technical Report No. 275, 1927.
12. ———: The Prediction of Airfoil Characteristics. N. A. C. A. Technical Report No. 312, 1929.
13. Higgins, George J., Diehl, W. S., and DeFoe, George L.: Tests on Models of Three British Airplanes in the Variable Density Wind Tunnel. N. A. C. A. Technical Report No. 279, 1928.

TABLE I.—VALUES FOR ASPECT RATIO 6

Airfoil	Page	C_L maximum	C_D minimum	L/D maximum	Thickness at—		$C.P.$ at—	
					0.15 chord	0.65 chord	$C_{L\ max}$	1/4 $C_{L\ max.}$
					Per cent chord		Per cent chord from L. E.	
N. A. C. A. 97	8	1.335	0.0123	18.2	13.30	8.16	33	59
N. A. C. A. 98	8	1.363	.0138	17.4	13.40	8.27	33	66
N. A. C. A. 99	9	1.060	.0103	18.4	12.06	8.13	22	23
N. A. C. A.–M1	9	.805	.0073	23.1	5.34	4.61	33	21
N. A. C. A.–M2	10	.903	.0050	21.9	6.98	6.01	26	21
N. A. C. A.–M3	10	1.080	.0094	20.3	10.28	8.81	26	17
N. A. C. A.–M4	11		.0071	24.2	5.41	4.74		
N. A. C. A.–M5	11	1.132	.0071	22.8	7.10	6.19	26	19
N. A. C. A.–M6	12	1.321	.0101	20.8	10.29	8.96	25	20
N. A. C. A.–M7	13	1.145	.0084	22.6	5.31	4.69	24	18
N. A. C. A.–M8	13	1.153	.0089	21.2	6.99	6.12	26	20
N. A. C. A.–M9	13	1.137	.0100	20.3	10.27	8.86	25	18
N. A. C. A.–M10	14	1.004	.0064	23.1	5.36	4.66	26	29
N. A. C. A.–M11	14	1.080	.0081	21.6	7.03	6.00	30	29
N. A. C. A.–M12	15	1.253	.0101	19.4	10.21	8.88	28	32
N. A. C. A.–M13	15	1.229	.0117	19.3	5.35	4.70	28	35
N. A. C. A.–M14	16	1.250	.0098	21.2	7.00	6.10	30	37
N. A. C. A.–M15	16	1.263	.0094	20.0	10.30	8.94	29	31
N. A. C. A.–M16	17	1.119	.0081	21.2	5.32	4.66	27	28
N. A. C. A.–M17	17		.0089	20.8	6.92	6.08		
N. A. C. A.–M18	18		.0095	19.9	10.30	8.92		
N. A. C. A.–M19	18	1.258	.0201	19.5	5.27	4.65	29	34
N. A. C. A.–M20	19	1.320	.0167	20.1	7.00	6.12	30	35
N. A. C. A.–M21	19		.0116	19.4	10.30	8.94		
N. A. C. A.–M22	20	1.230	.0181	20.2	5.38	4.76	30	27
N. A. C. A.–M23	20		.0160	20.3	6.98	6.14		
N. A. C. A.–M24	21		.0122	18.5	10.28	8.86		
N. A. C. A.–M25	21	1.237	.0380	15.3	5.38	4.76	31	35
N. A. C. A.–M26	22	1.197	.0299	17.0	6.93	6.08	34	36
N. A. C. A.–M27	22		.0193	17.0	10.26	8.94		
U. S. A. 5	23	1.200	.0117	22.6	6.05	4.80	32	56
U. S. A. 27	23	1.386	.0115	20.8	10.40	8.64	31	48
U. S. A. 35A	24	1.203	.0145	18.6	16.60	11.84	36	64
U. S. A. 35B	24	1.374	.0092	20.6	10.56	7.51	31	41
R. A. F. 15	25	1.209	.0050	24.8	6.38	5.02	29	40
Göttingen 387	25	1.328	.0123	18.2	13.83	9.84	33	51
Clark Y	26	1.420	.0108	21.1	10.51	8.24	29	45
U. S. N. P. S. 1	26	.933	.0092	27.0	3.58	3.22	35	30
U. S. N. P. S. 2	27	1.215	.0173	20.1	7.16	6.44	31	43
U. S. N. P. S. 3	27	1.438	.0210	17.9	8.95	8.05	31	44
U. S. N. P. S. 4	28	1.492	.0221	17.5	10.74	9.66	33	49
U. S. N. P. S. 5	28	1.376	.0263	15.7	14.32	12.88	33	58
U. S. N. P. S. 6	29	1.181	.0280	13.6	17.90	16.10	34	74
N. A. C. A. CYH	29	1.302	.0111	20.4	10.54	8.30	28	33
R. A. F. 19	30	1.528	.0285	16.6	10.5	5.0	39	72

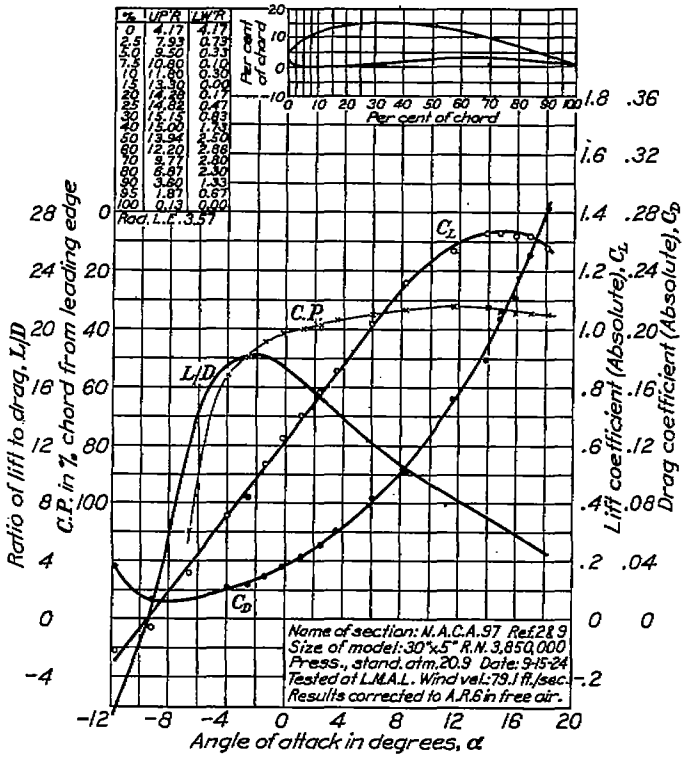

FIGURE 2.—N. A. C. A. 97 airfoil characteristics corrected to aspect ratio 6

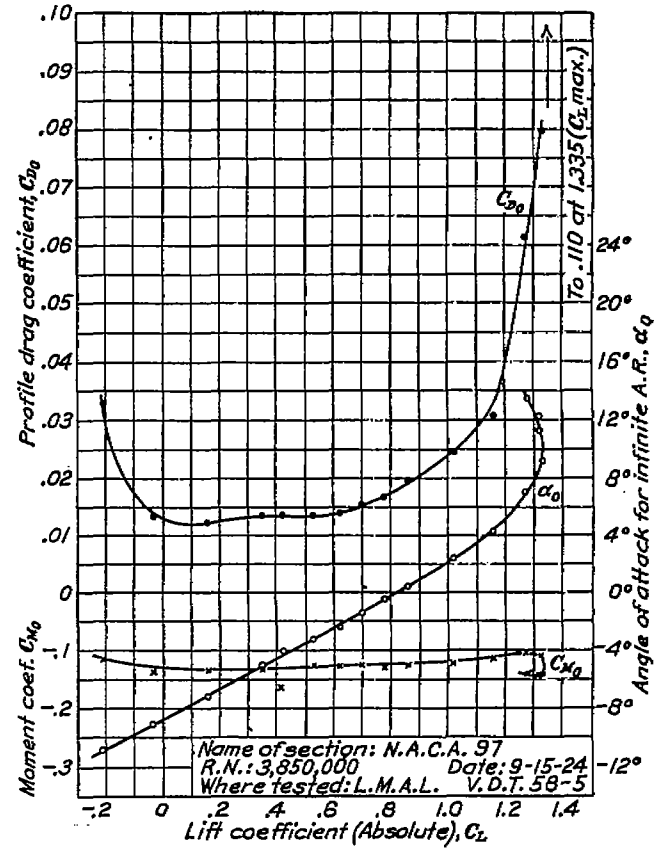

FIGURE 3.—N. A. C. A. 97 airfoil characteristics corrected to infinite aspect ratio

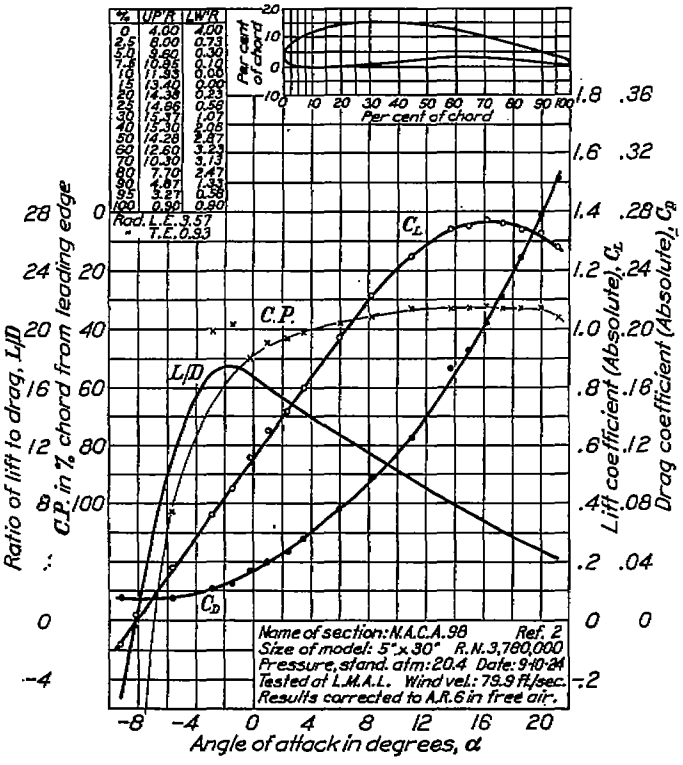

FIGURE 4.—N. A. C. A. 98 airfoil characteristics corrected to aspect ratio 6

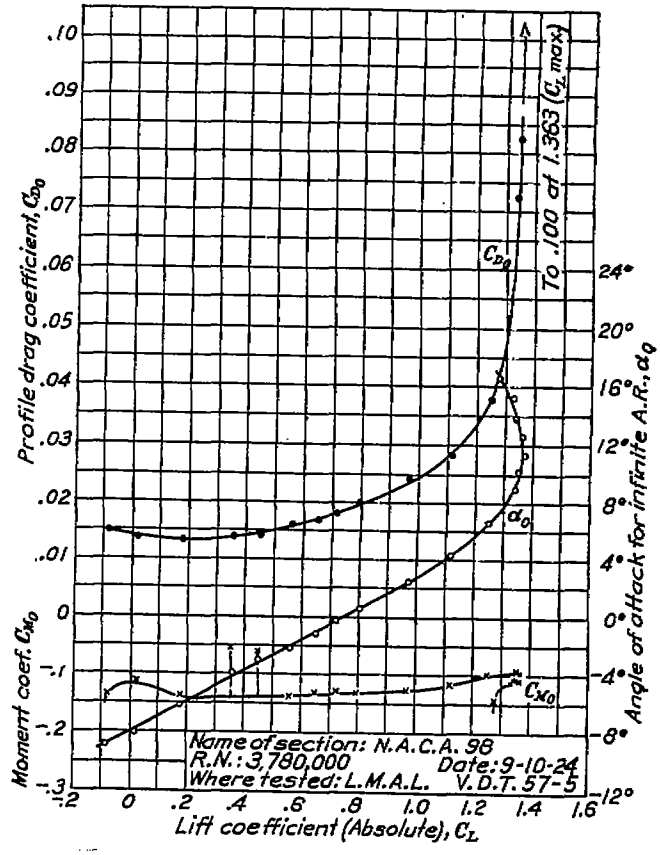

FIGURE 5.—N. A. C. A. 98 airfoil characteristics corrected to infinite aspect ratio

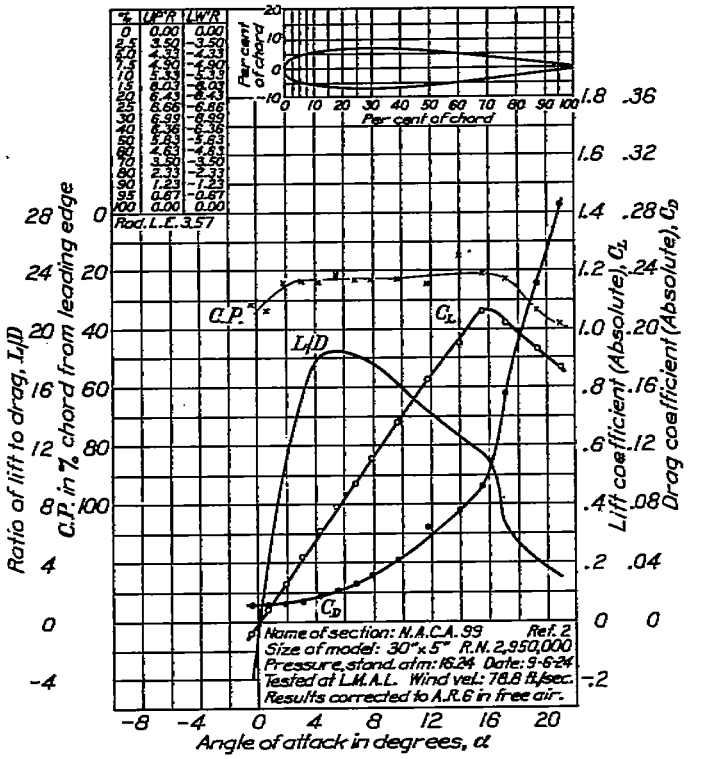

FIGURE 6.—N. A. C. A. 99 airfoil characteristics corrected to aspect ratio 6

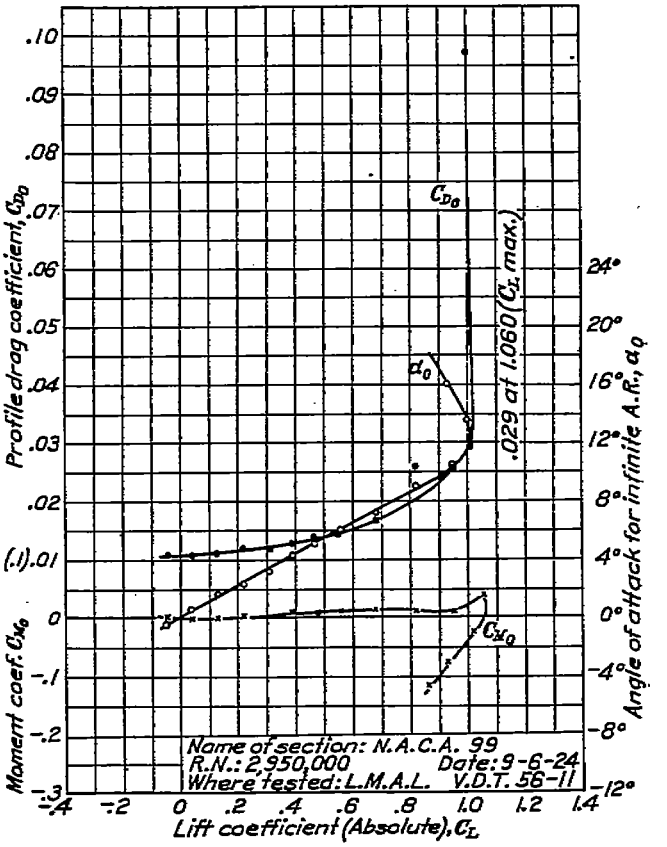

FIGURE 7.—N. A. C. A. 99 airfoil characteristics corrected to infinite aspect ratio

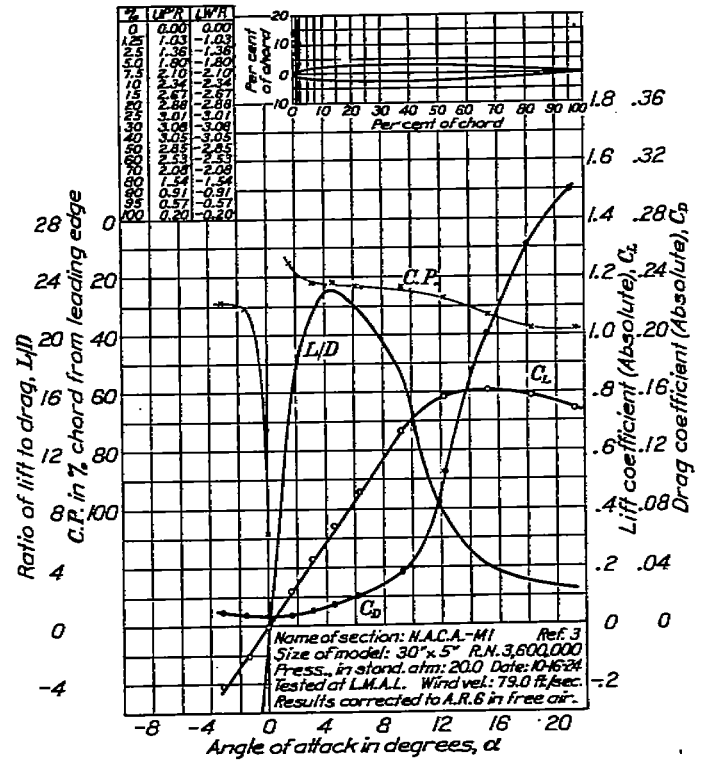

FIGURE 8.—N. A. C. A.-M1 airfoil characteristics corrected to aspect ratio 6

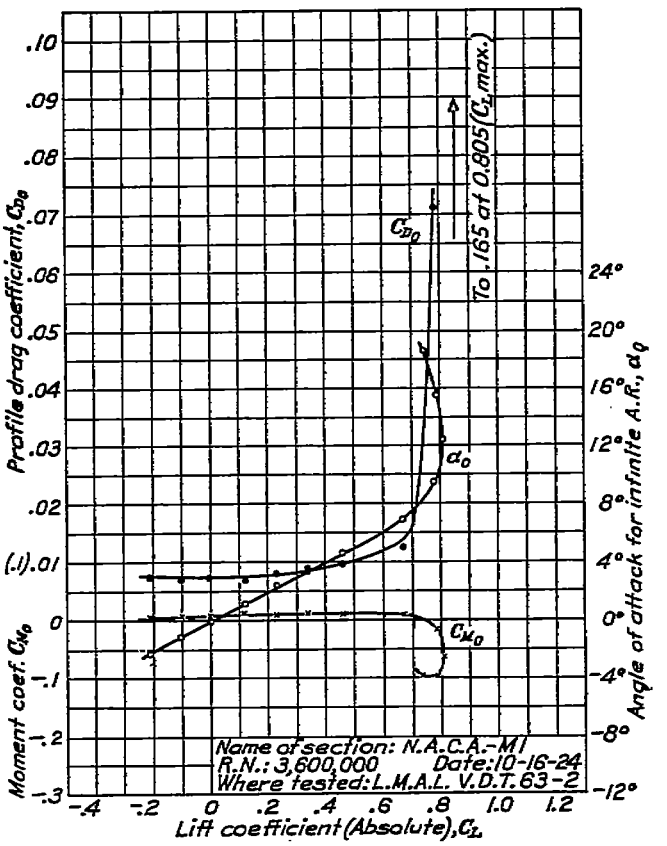

FIGURE 9.—N. A. C. A.-M1 airfoil characteristics corrected to infinite aspect ratio

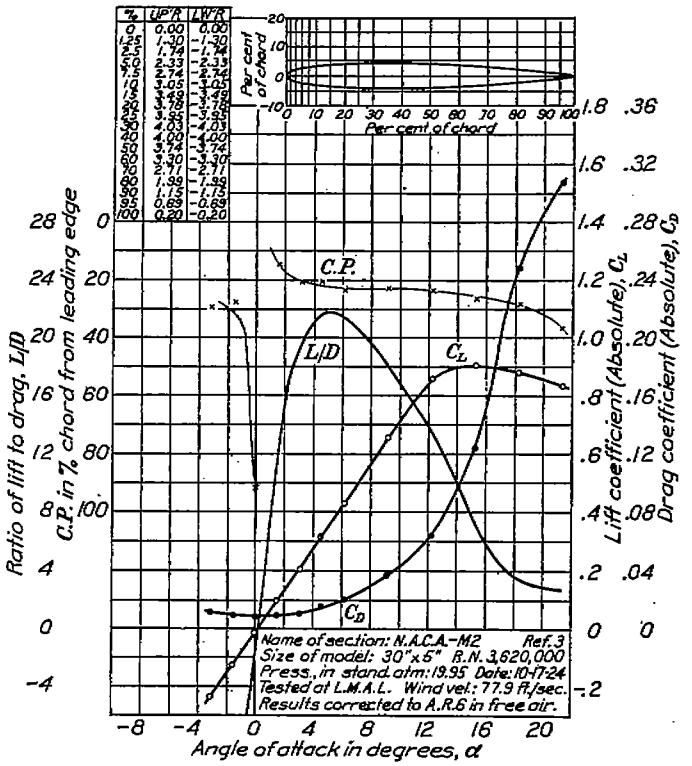

FIGURE 10.—N. A. C. A.-M2 airfoil characteristics corrected to aspect ratio 6

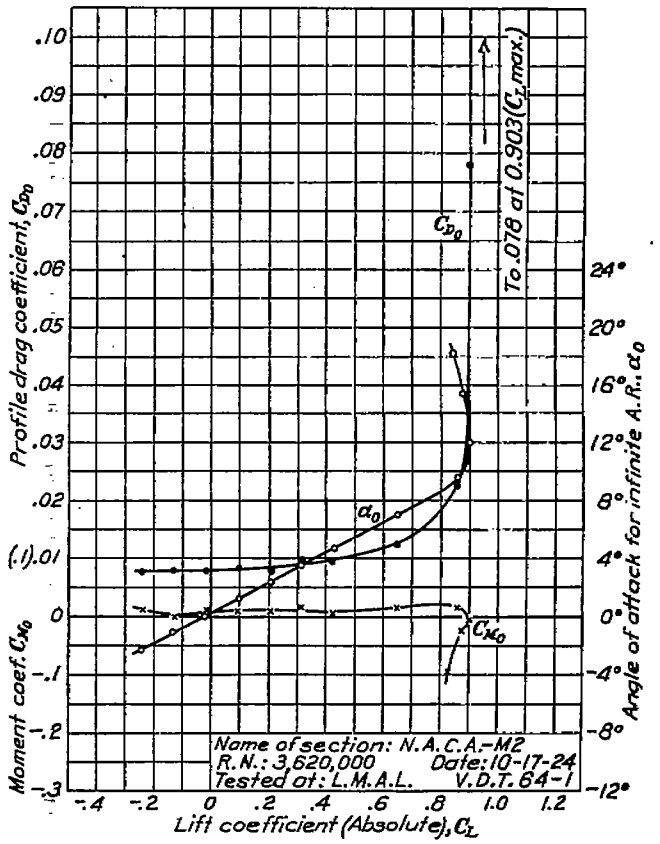

FIGURE 11.—N. A. C. A.-M2 airfoil characteristics corrected to infinite aspect ratio

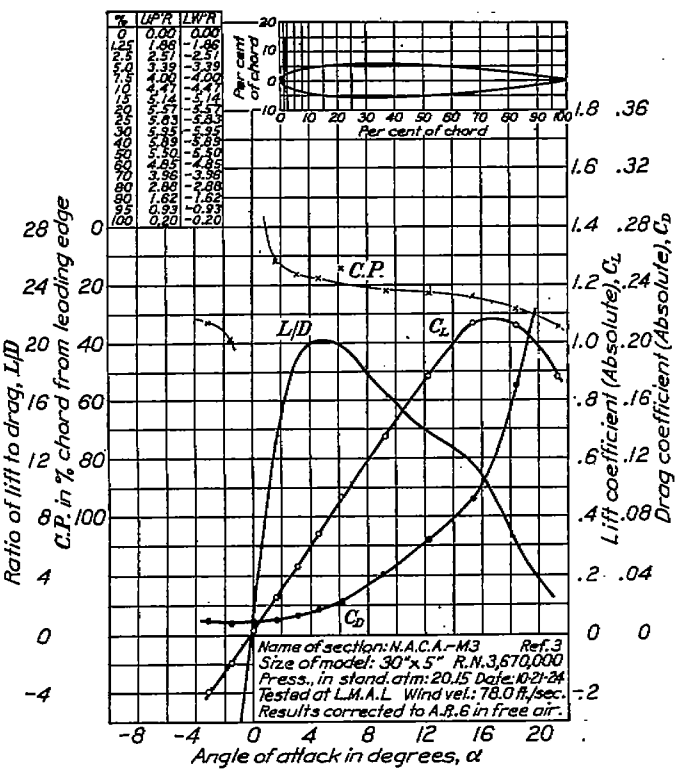

FIGURE 12.—N. A. C. A.-M3 airfoil characteristics corrected to aspect ratio 6

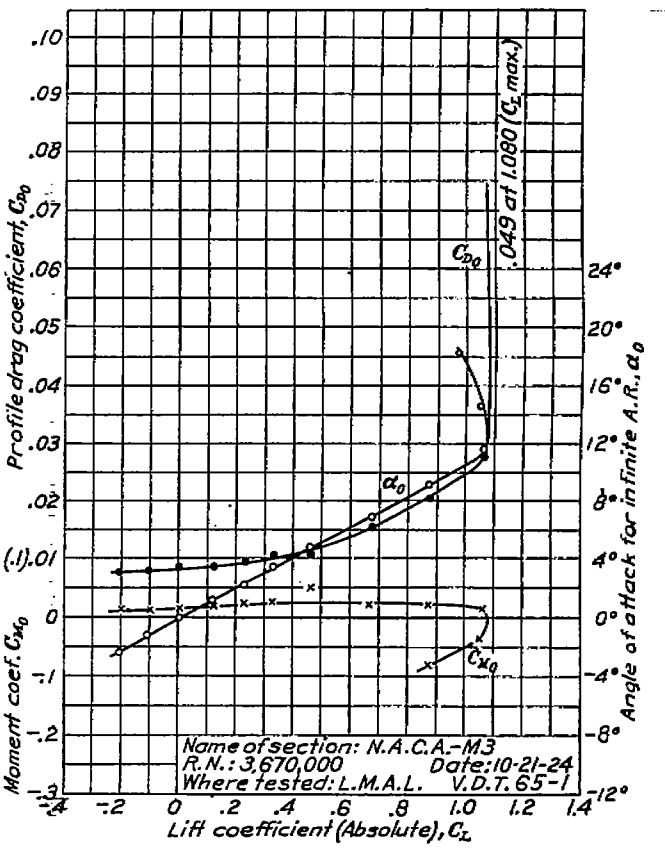

FIGURE 13.—N. A. C. A.-M3 airfoil characteristics corrected to infinite aspect ratio

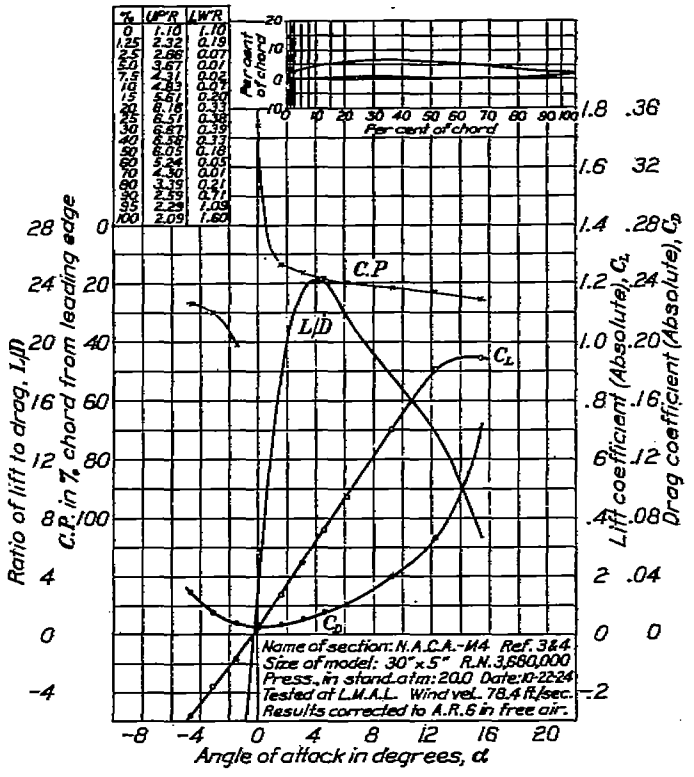

FIGURE 14.—N. A. C. A.-M4 airfoil characteristics corrected to aspect ratio 6

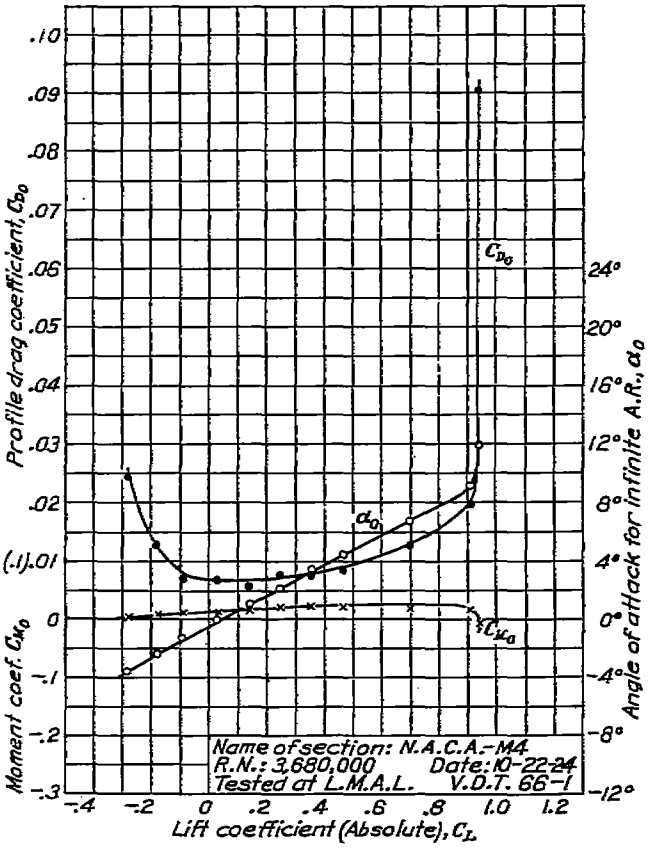

FIGURE 15.—N. A. C. A.-M4 airfoil characteristics corrected to infinite aspect ratio

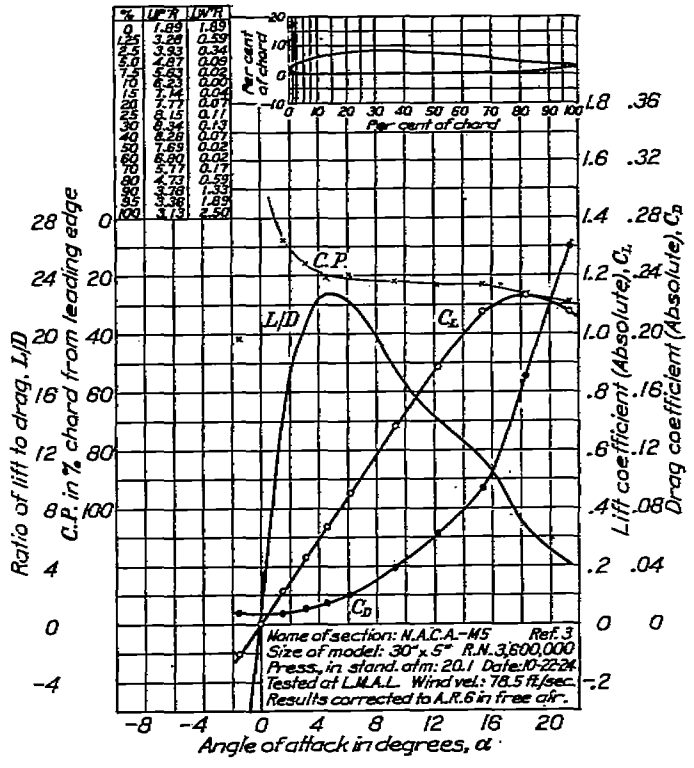

FIGURE 16.—N. A. C. A.-M5 airfoil characteristics corrected to aspect ratio 6

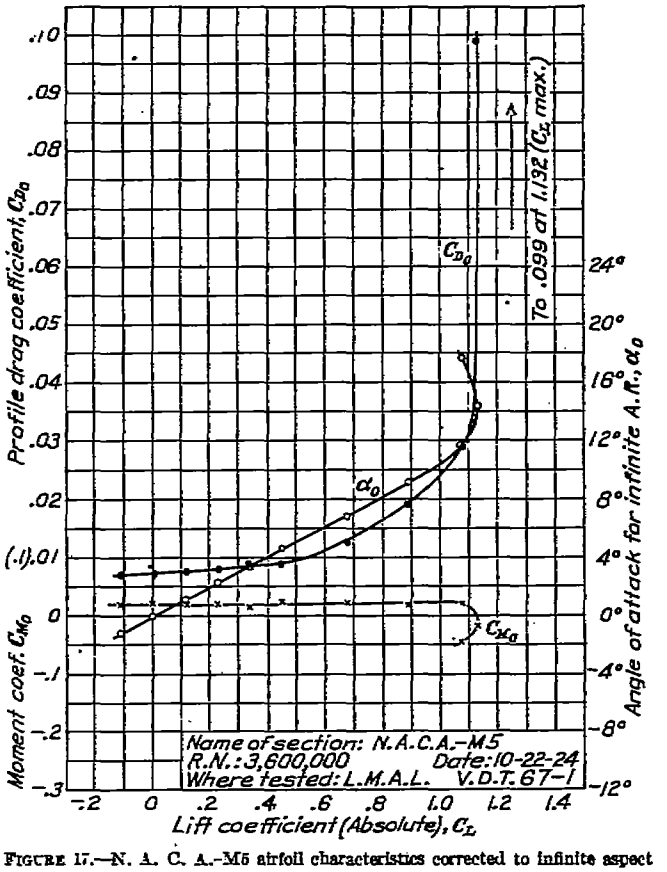

FIGURE 17.—N. A. C. A.-M5 airfoil characteristics corrected to infinite aspect ratio

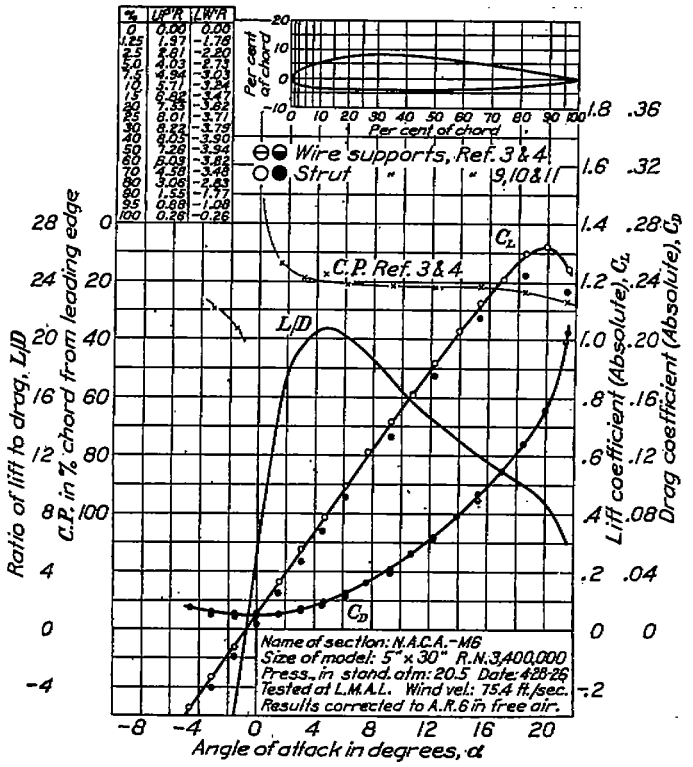

FIGURE 18.—N. A. C. A.-M6 airfoil characteristics corrected to aspect ratio 6

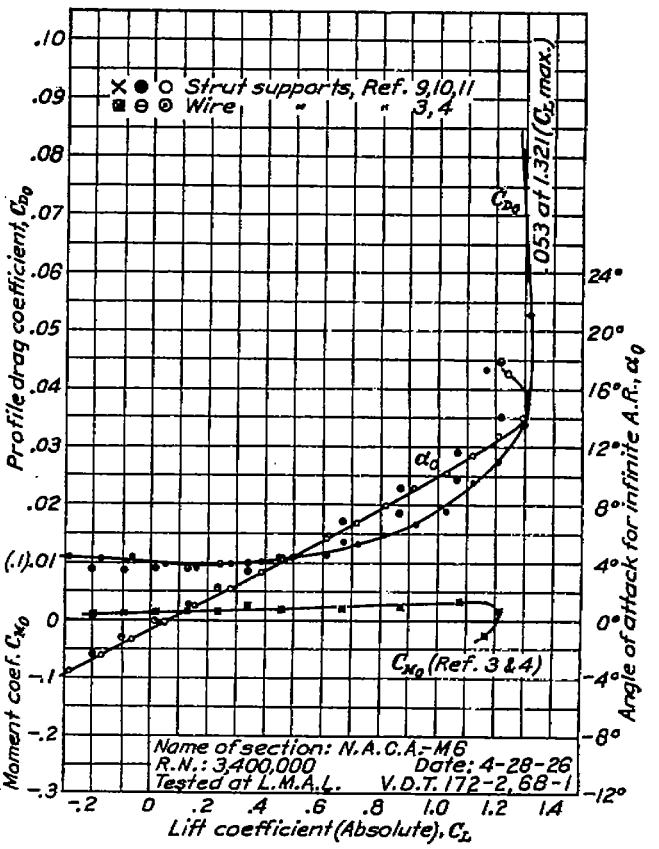

FIGURE 19.—N. A. C. A.-M6 airfoil characteristics corrected to infinite aspect ratio

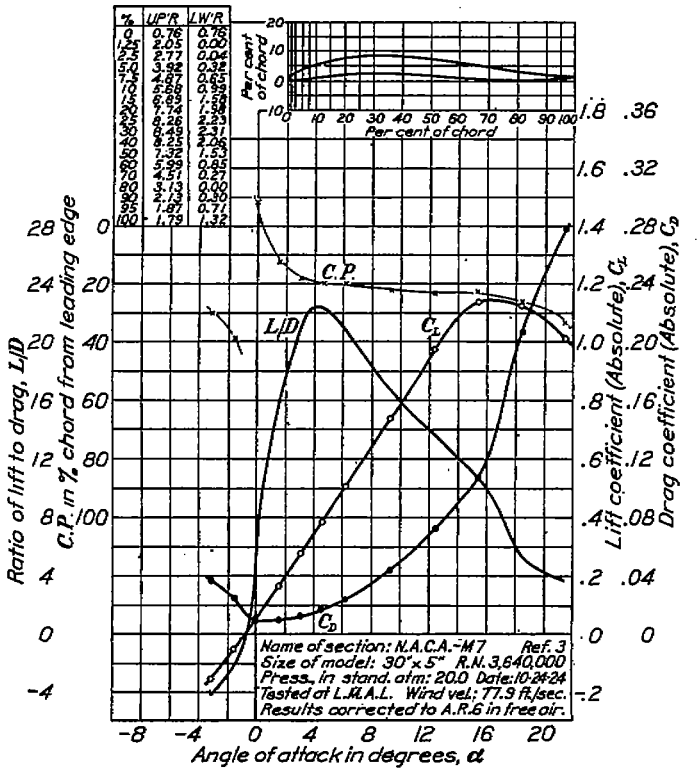

FIGURE 20.—N. A. C. A.-M7 airfoil characteristics corrected to aspect ratio 6

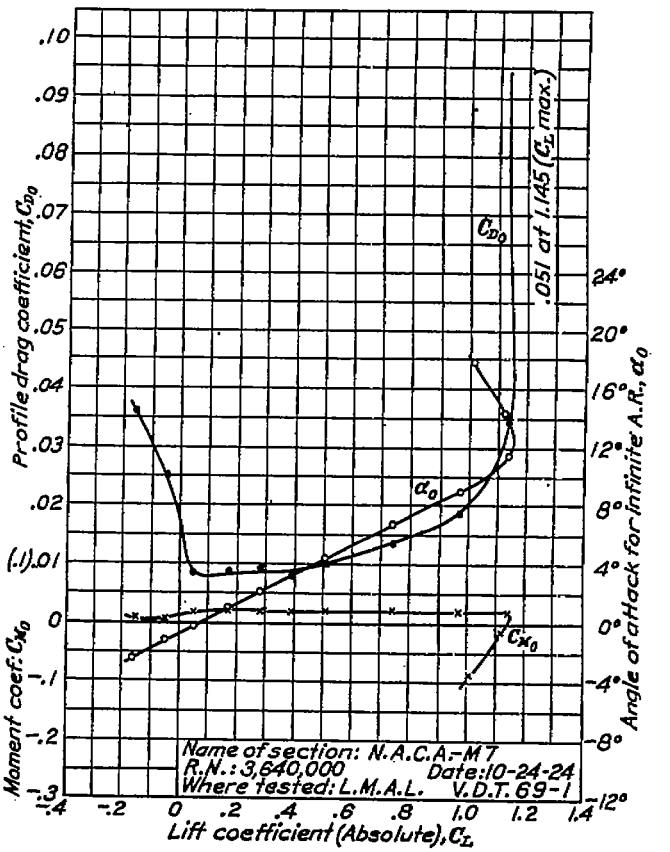

FIGURE 21.—N. A. C. A.-M7 airfoil characteristics corrected to infinite aspect ratio

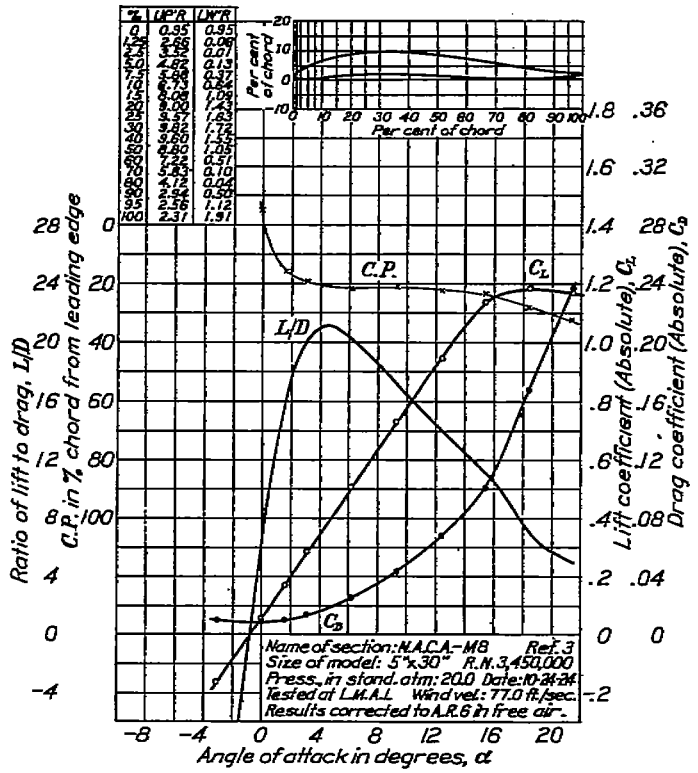

FIGURE 22.—N. A. C. A.-M8 airfoil characteristics corrected to aspect ratio 6

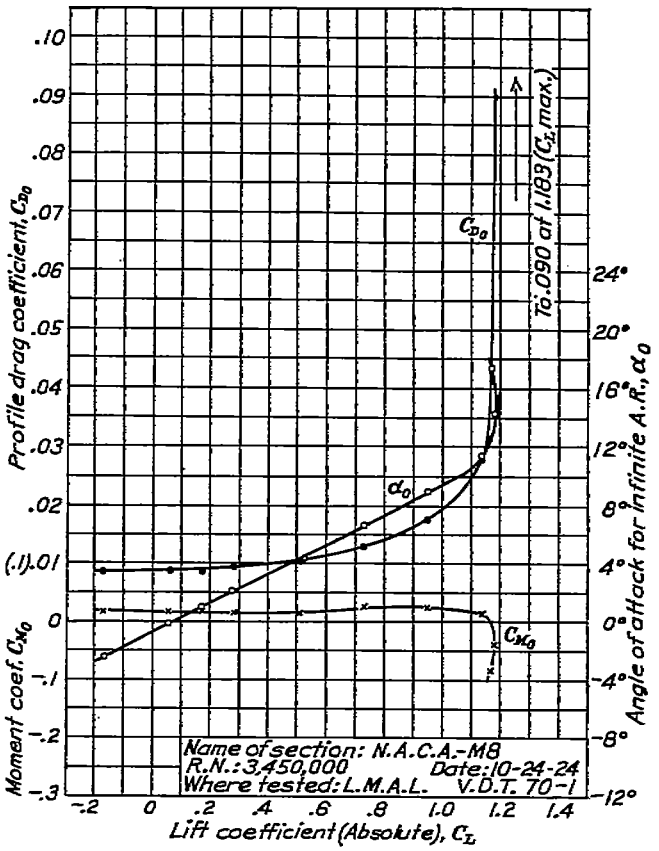

FIGURE 23.—N. A. C. A.-M8 airfoil characteristics corrected to infinite aspect ratio

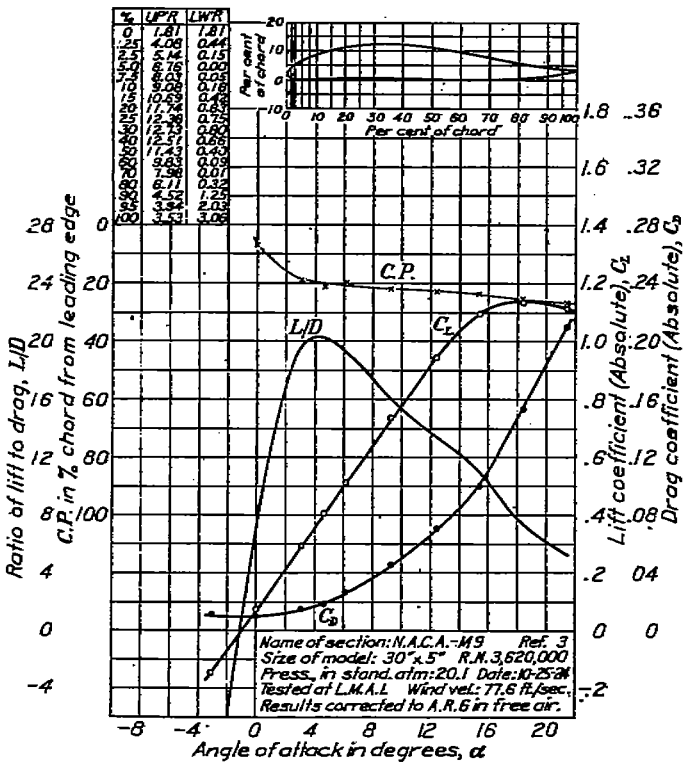

FIGURE 24.—N. A. C. A.-M9 airfoil characteristics corrected to aspect ratio 6

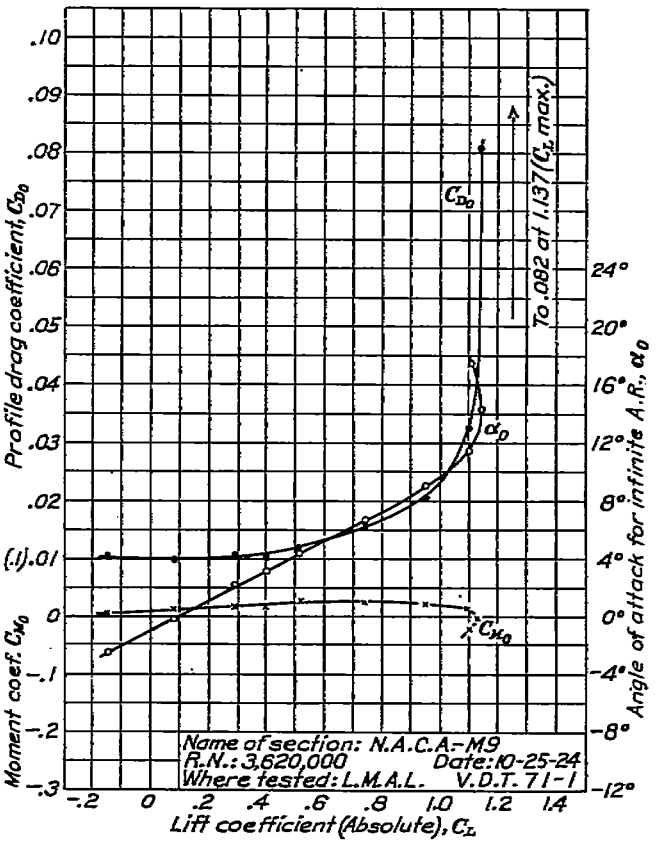

FIGURE 25.—N. A. C. A.-M9 airfoil characteristics corrected to infinite aspect ratio

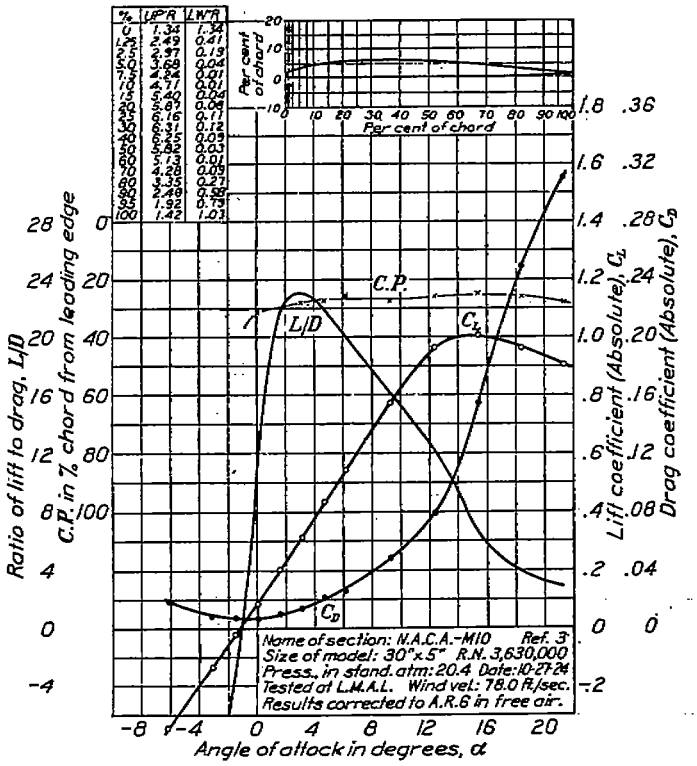

FIGURE 26.—N. A. C. A.-M10 airfoil characteristics corrected to aspect ratio 6

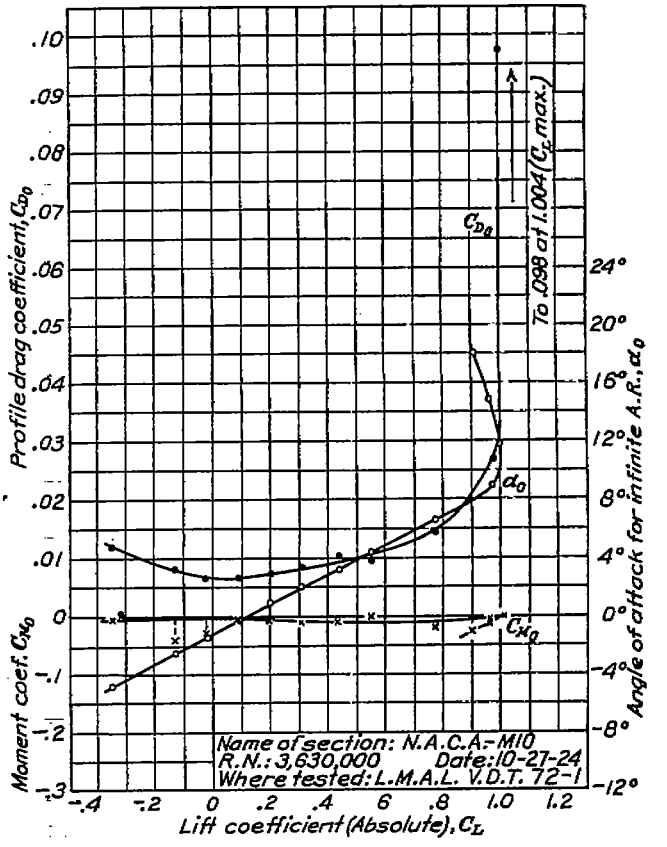

FIGURE 27.—N. A. C. A.-M10 airfoil characteristics corrected to infinite aspect ratio

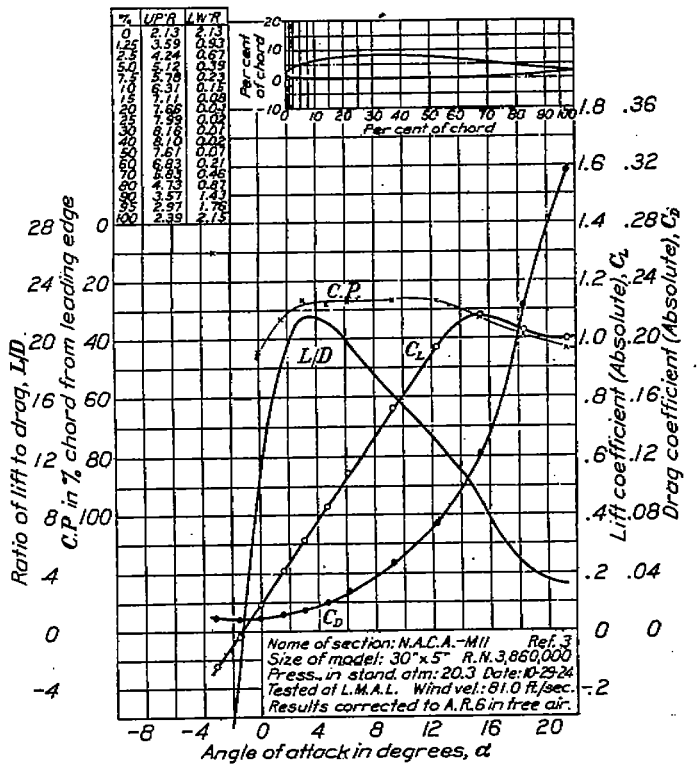

FIGURE 28.—N. A. C. A.-M11 airfoil characteristics corrected to aspect ratio 6

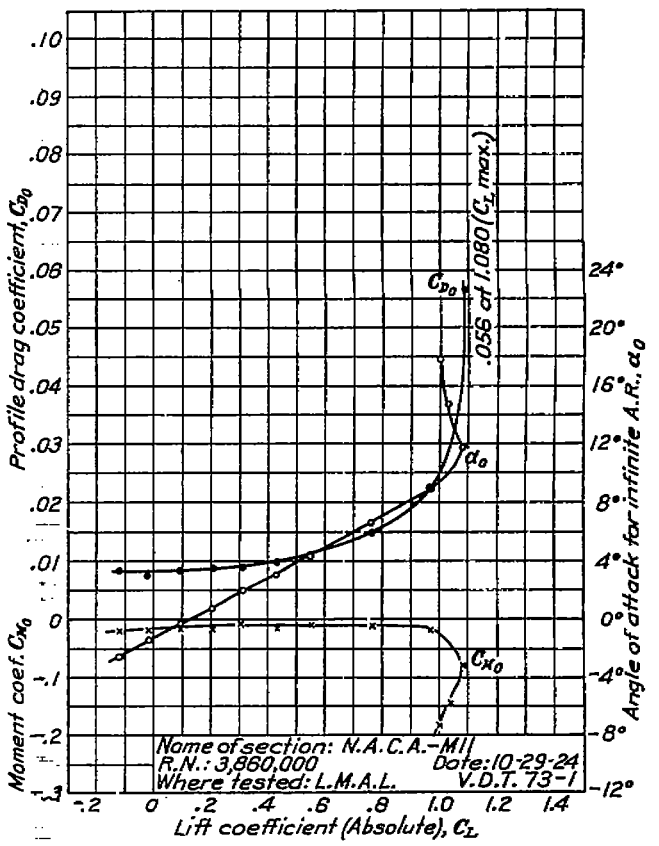

FIGURE 29.—N. A. C. A.-M11 airfoil characteristics corrected to infinite aspect ratio

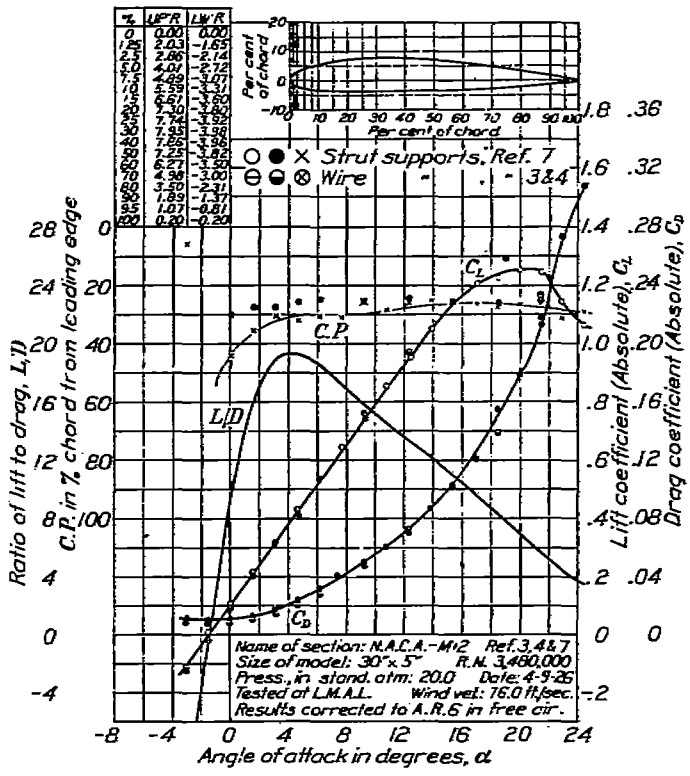

FIGURE 30.—N. A. C. A.-M12 airfoil characteristics corrected to aspect ratio 6

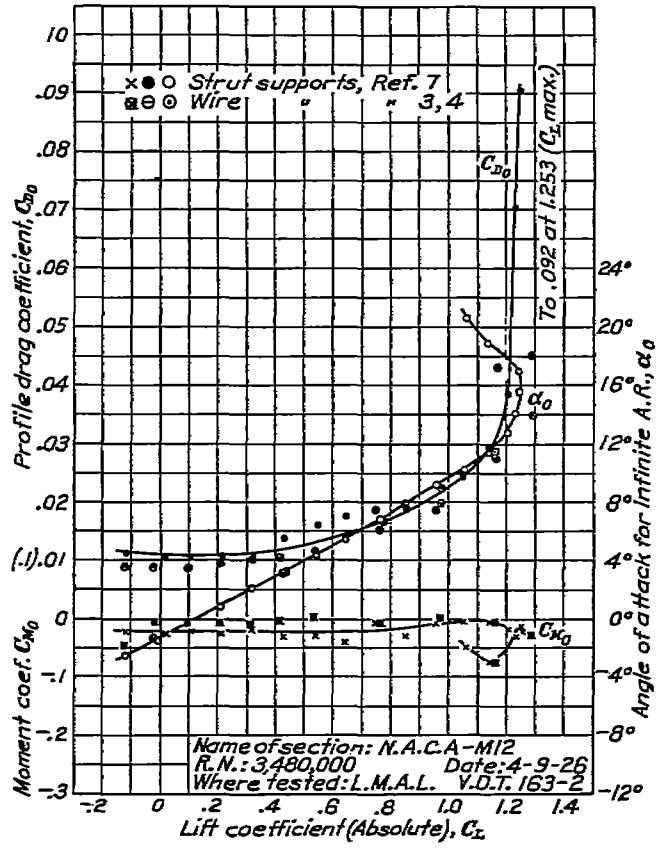

FIGURE 31.—N. A. C. A.-M12 airfoil characteristics corrected to infinite aspect ratio

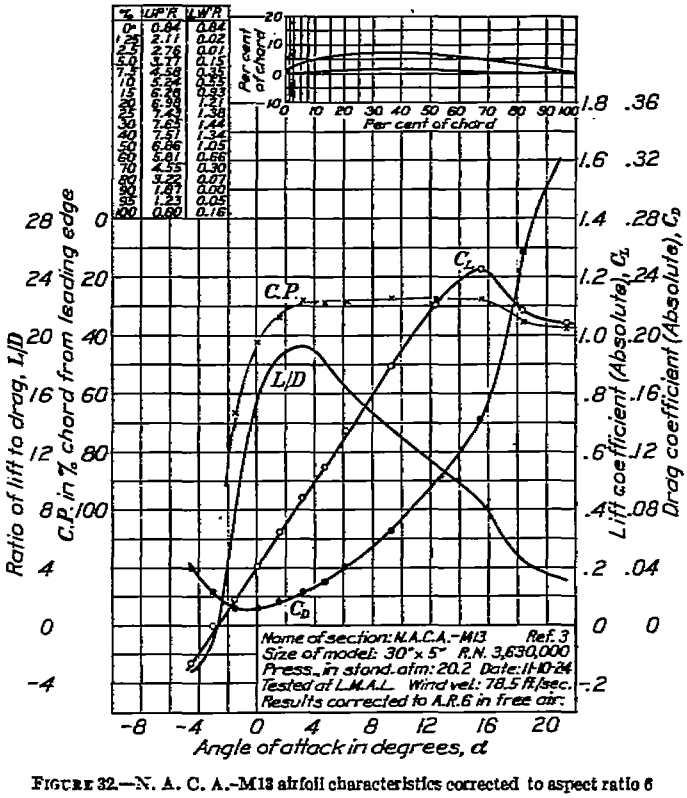

FIGURE 32.—N. A. C. A.-M13 airfoil characteristics corrected to aspect ratio 6

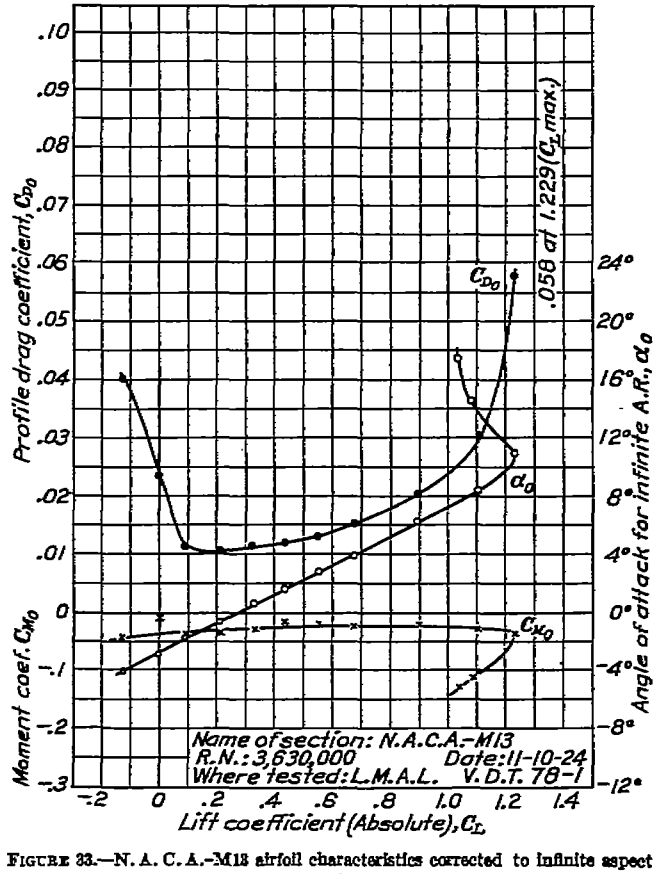

FIGURE 33.—N. A. C. A.-M13 airfoil characteristics corrected to infinite aspect ratio

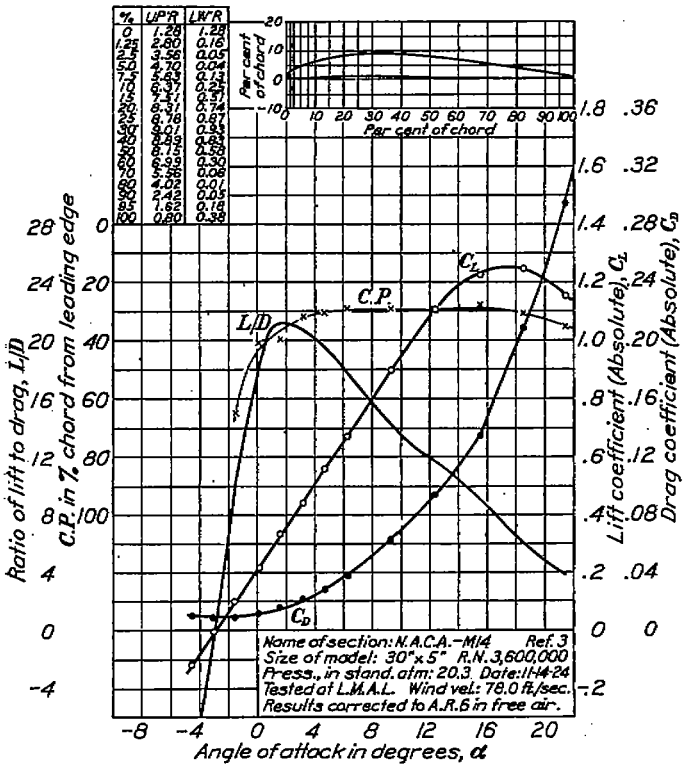

FIGURE 34.—N. A. C. A.-M14 airfoil characteristics corrected to aspect ratio 6

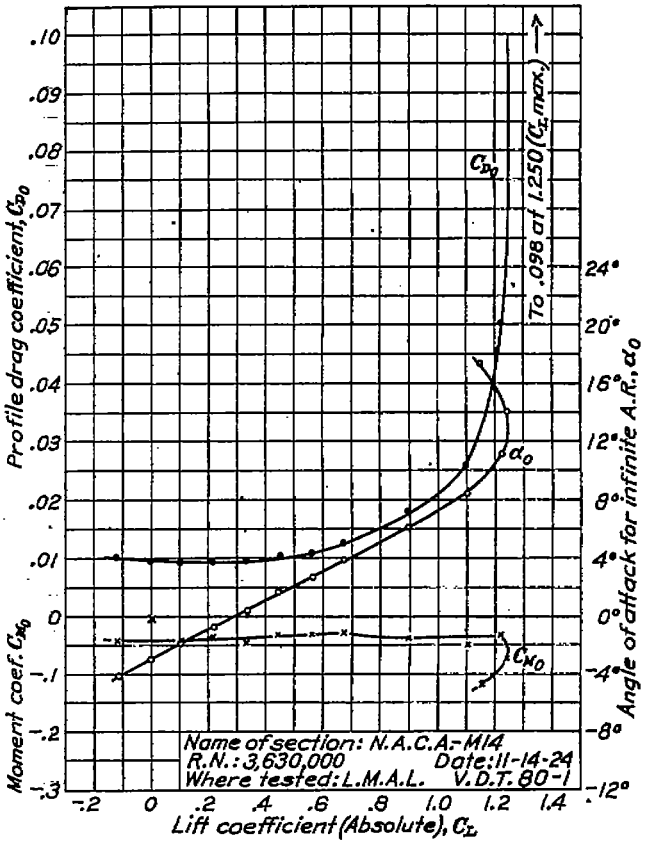

FIGURE 35.—N. A. C. A.-M14 airfoil characteristics corrected to infinite aspect ratio

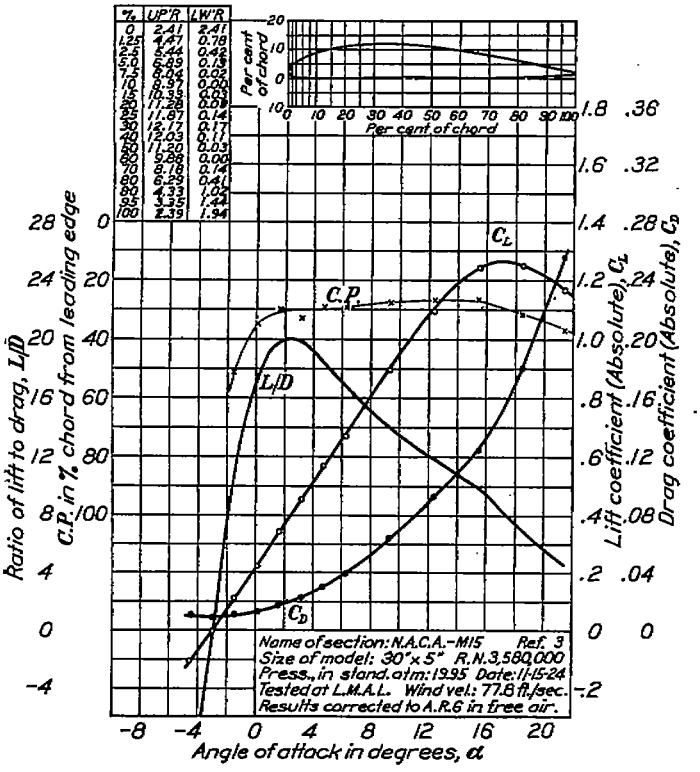

FIGURE 36.—N. A. C. A.-M15 airfoil characteristics corrected to aspect ratio 6

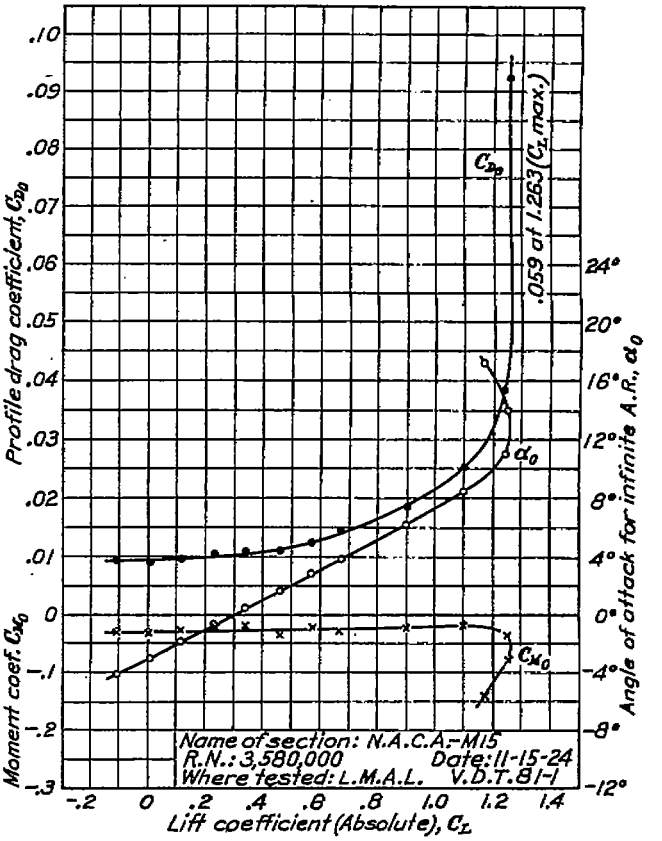

FIGURE 37.—N. A. C. A.-M15 airfoil characteristics corrected to infinite aspect ratio

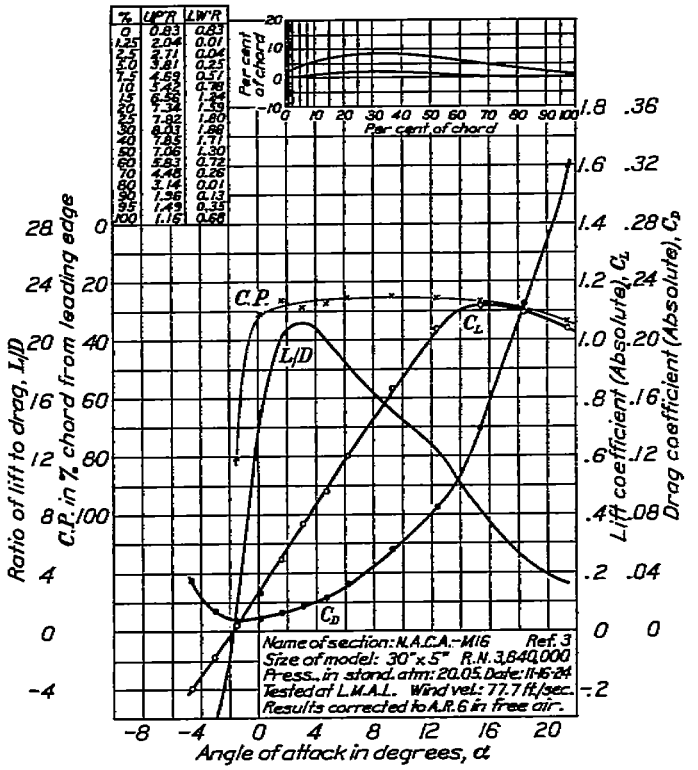

FIGURE 38.—N. A. C. A.-M16 airfoil characteristics corrected to aspect ratio 6

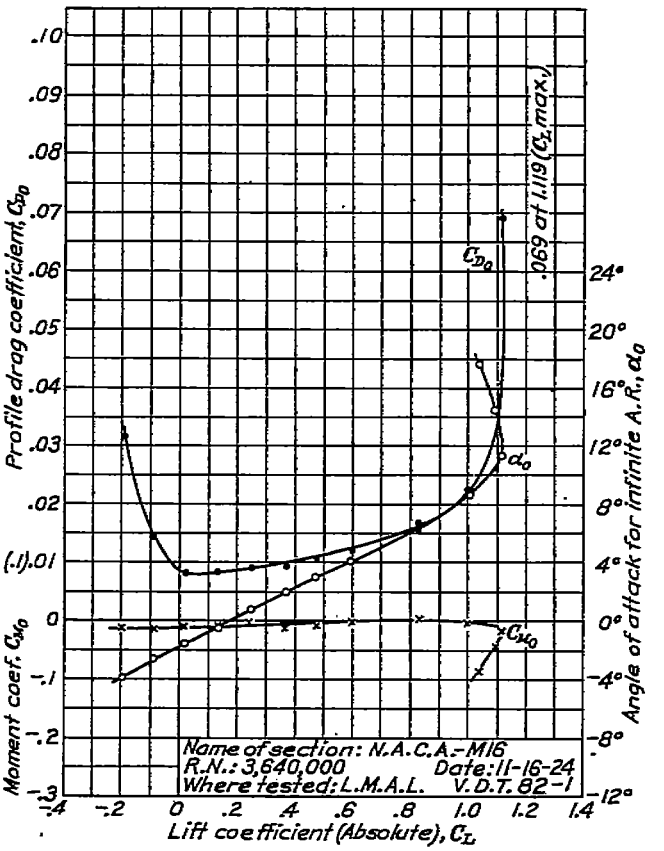

FIGURE 39.—N. A. C. A.-M16 airfoil characteristics corrected to infinite aspect ratio

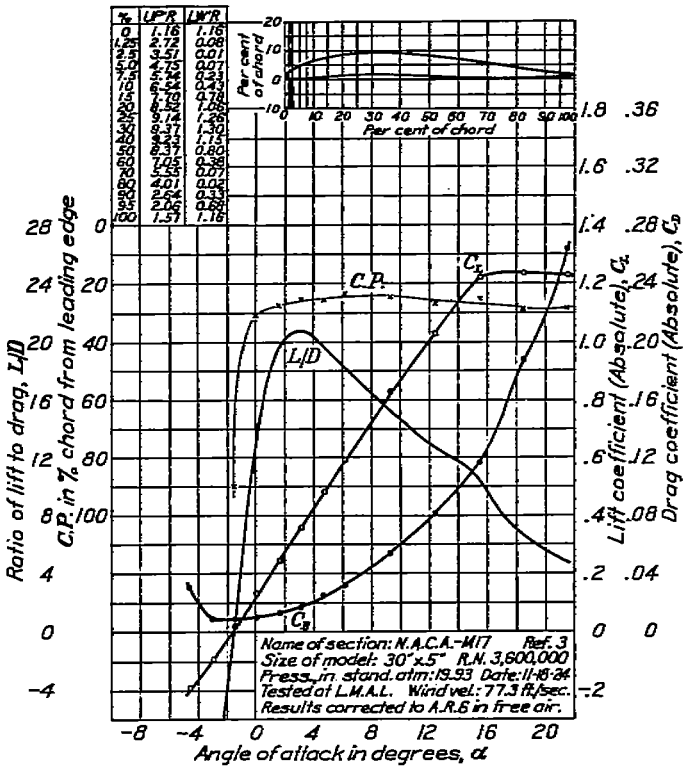

FIGURE 40.—N. A. C. A.-M17 airfoil characteristics corrected to aspect ratio 6

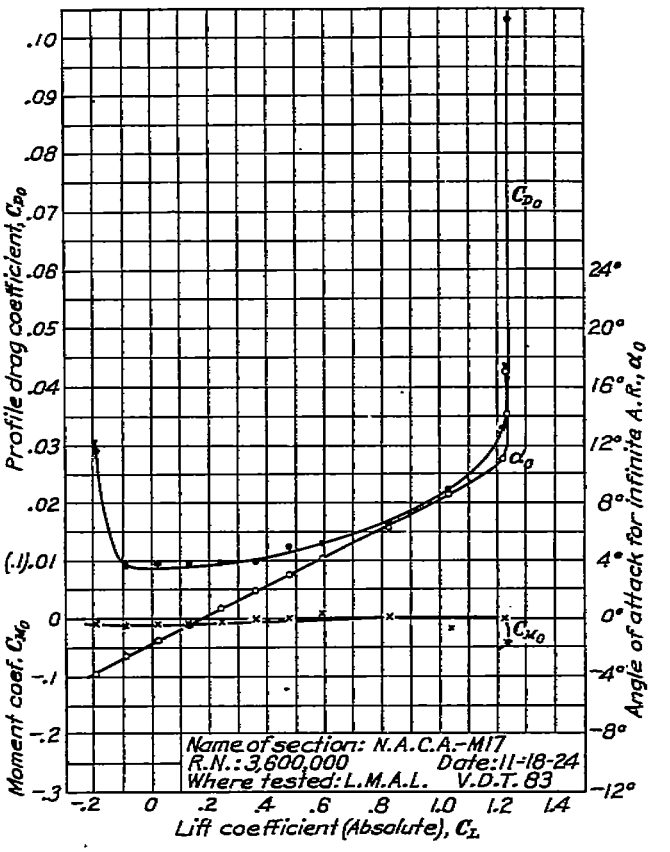

FIGURE 41.—N. A. C. A.-M17 airfoil characteristics corrected to infinite aspect ratio

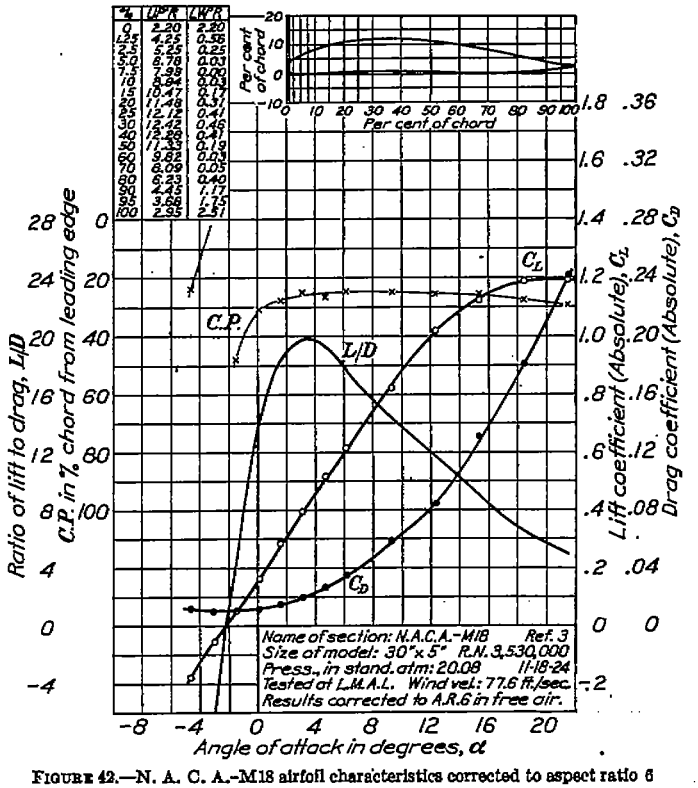

FIGURE 42.—N. A. C. A.-M18 airfoil characteristics corrected to aspect ratio 6

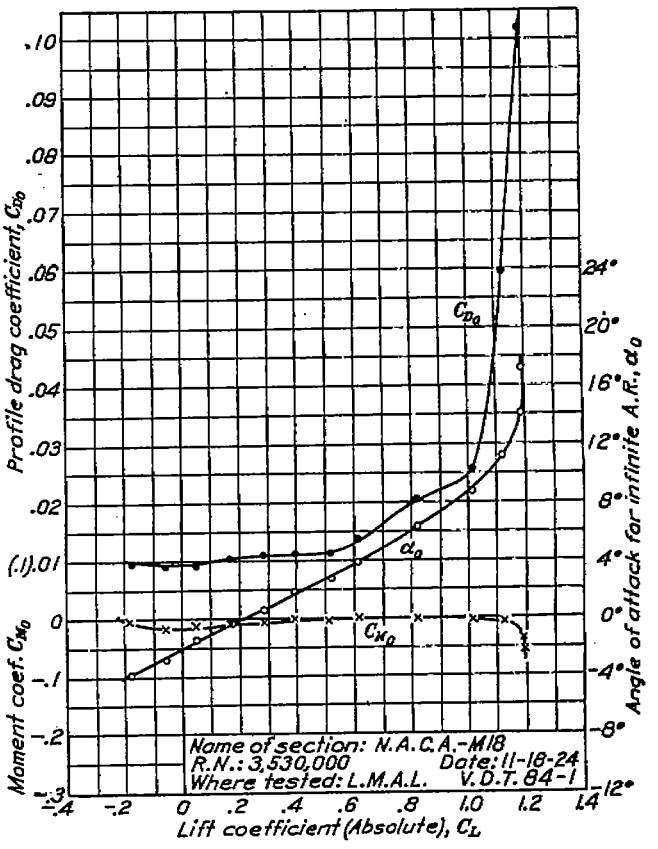

FIGURE 43.—N. A. C. A.-M18 airfoil characteristics corrected to infinite aspect ratio

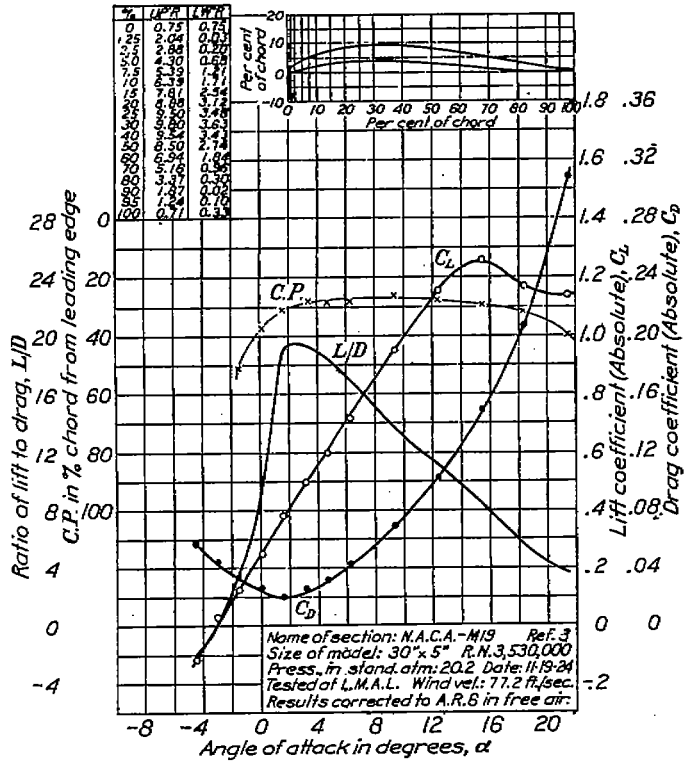

FIGURE 44.—N. A. C. A.-M19 airfoil characteristics corrected to aspect ratio 6

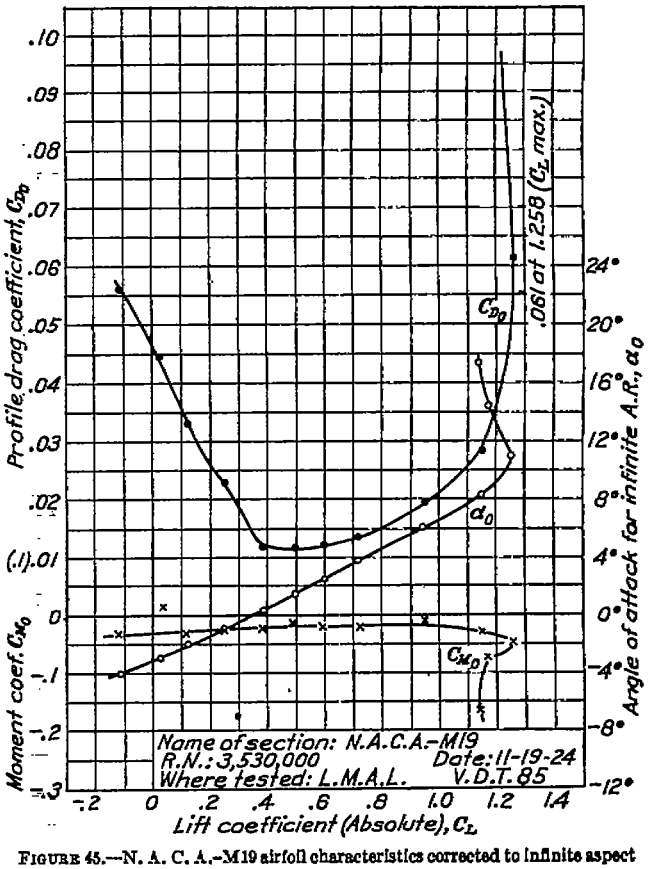

FIGURE 45.—N. A. C. A.-M19 airfoil characteristics corrected to infinite aspect ratio

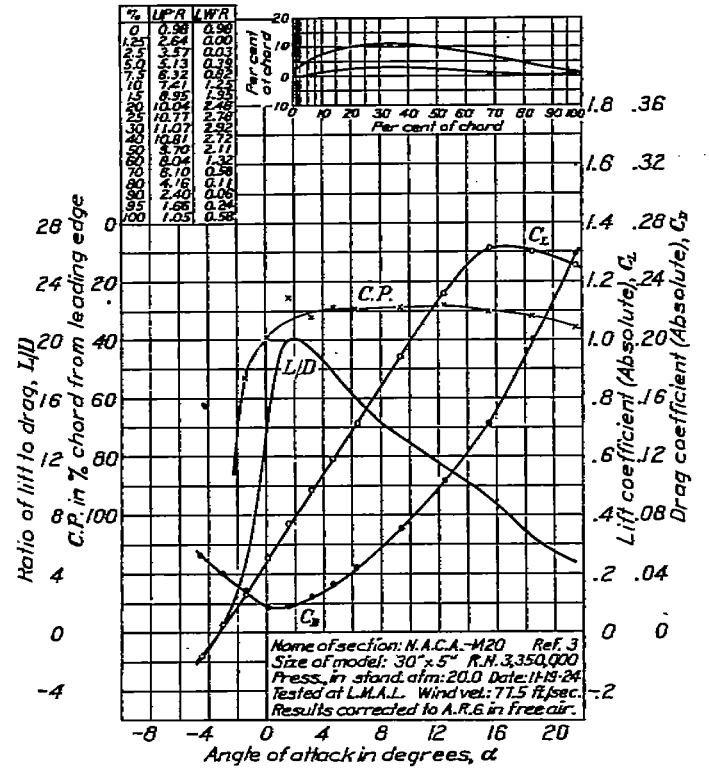

FIGURE 46.—N. A. C. A.-M20 airfoil characteristics corrected to aspect ratio 6

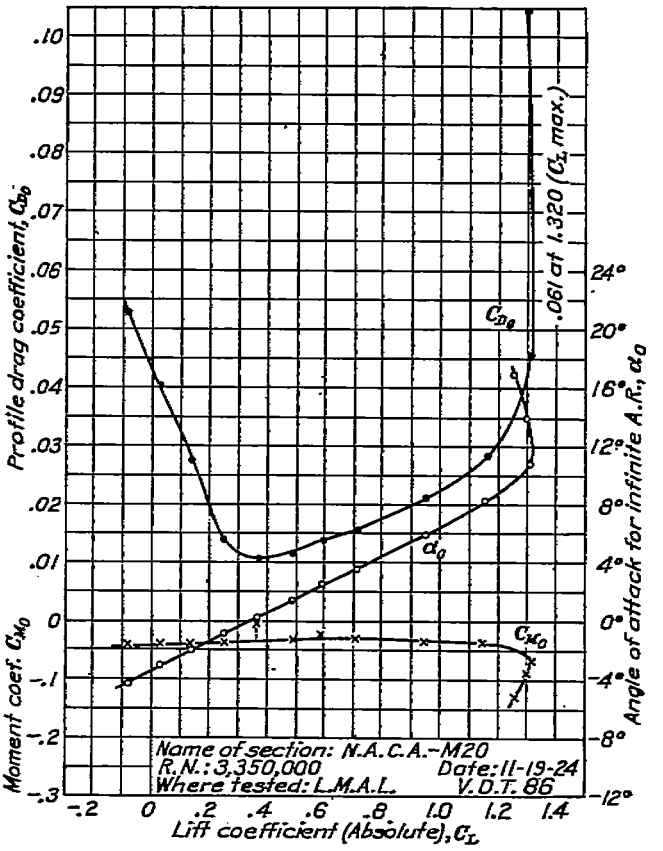

FIGURE 47.—N. A. C. A.-M20 airfoil characteristics corrected to infinite aspect ratio

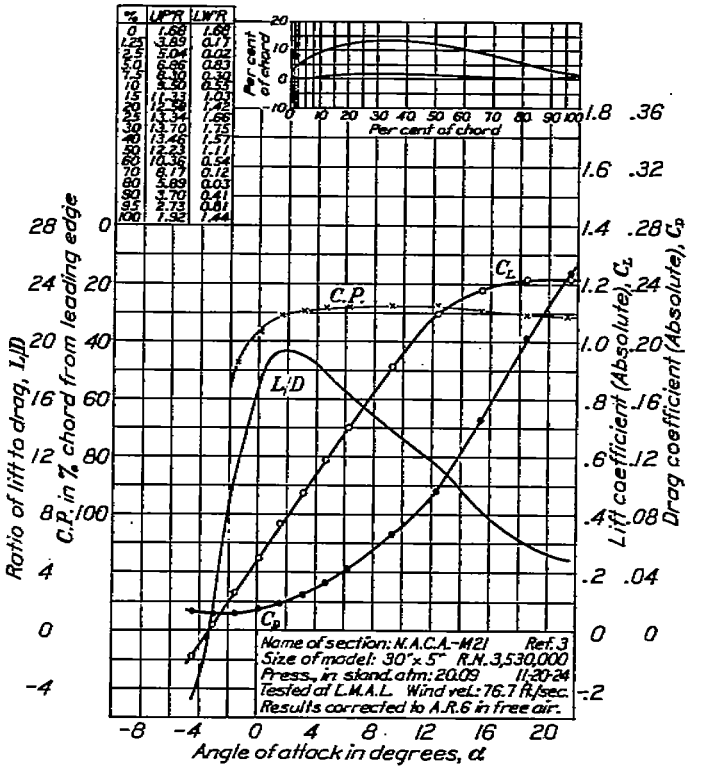

FIGURE 48.—N. A. C. A.-M21 airfoil characteristics corrected to aspect ratio 6

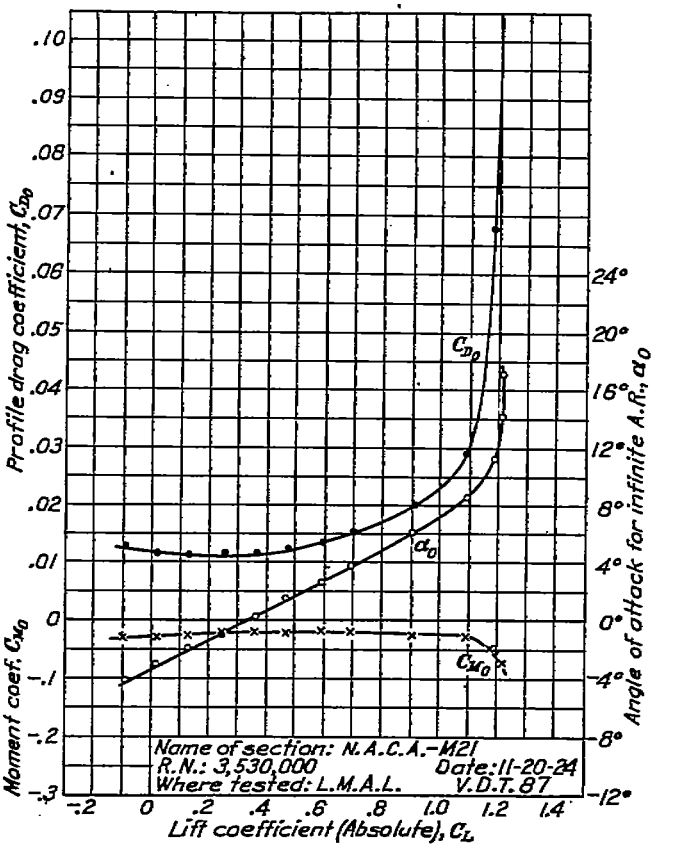

FIGURE 49.—N. A. C. A.-M21 airfoil characteristics corrected to infinite aspect ratio

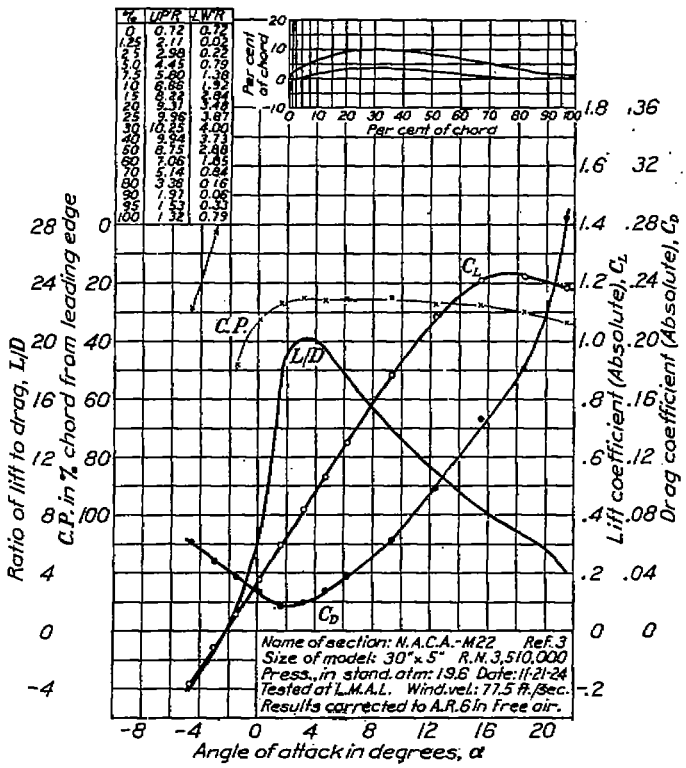

FIGURE 50.—N. A. C. A.-M22 airfoil characteristics corrected to aspect ratio 6

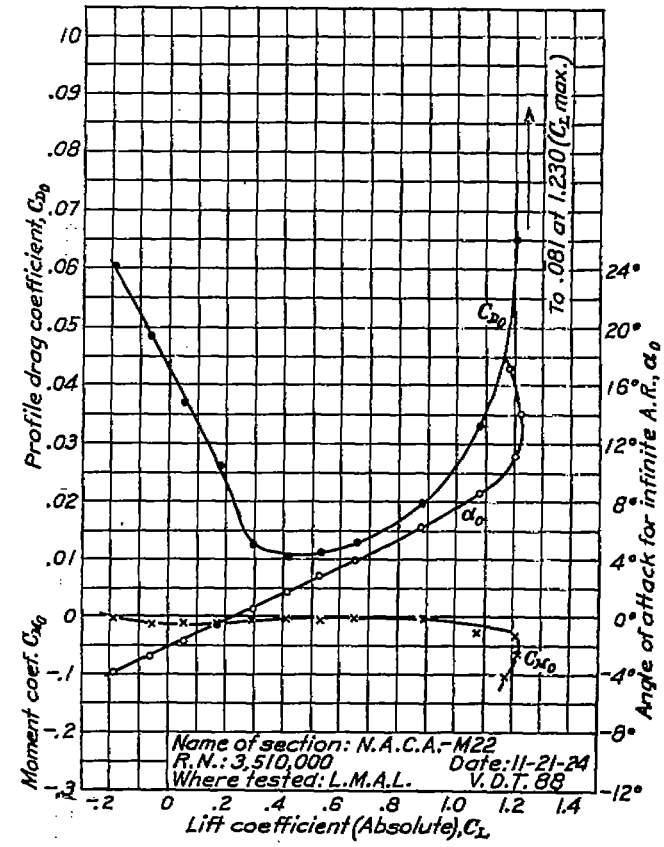

FIGURE 51.—N. A. C. A.-M22 airfoil characteristics corrected to infinite aspect ratio

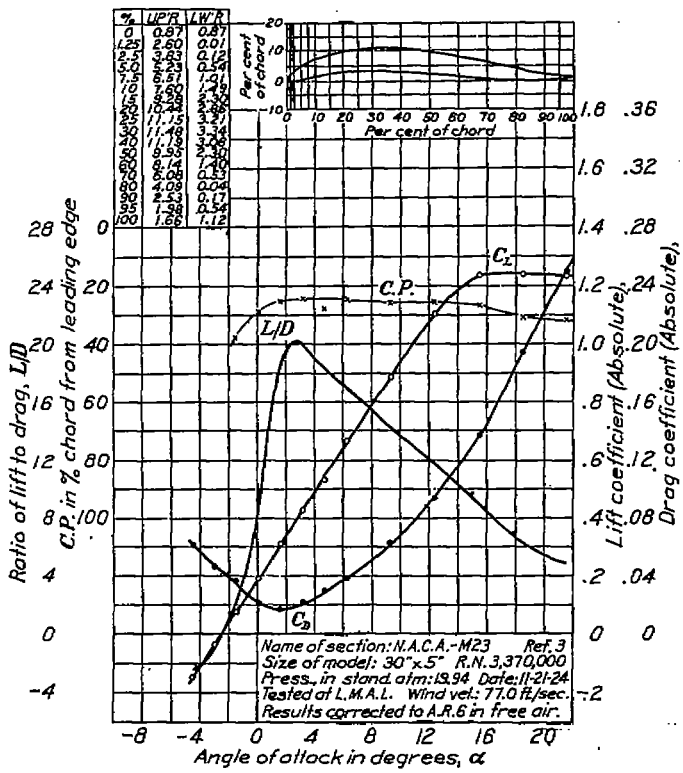

FIGURE 52.—N. A. C. A.-M23 airfoil characteristics corrected to aspect ratio 6

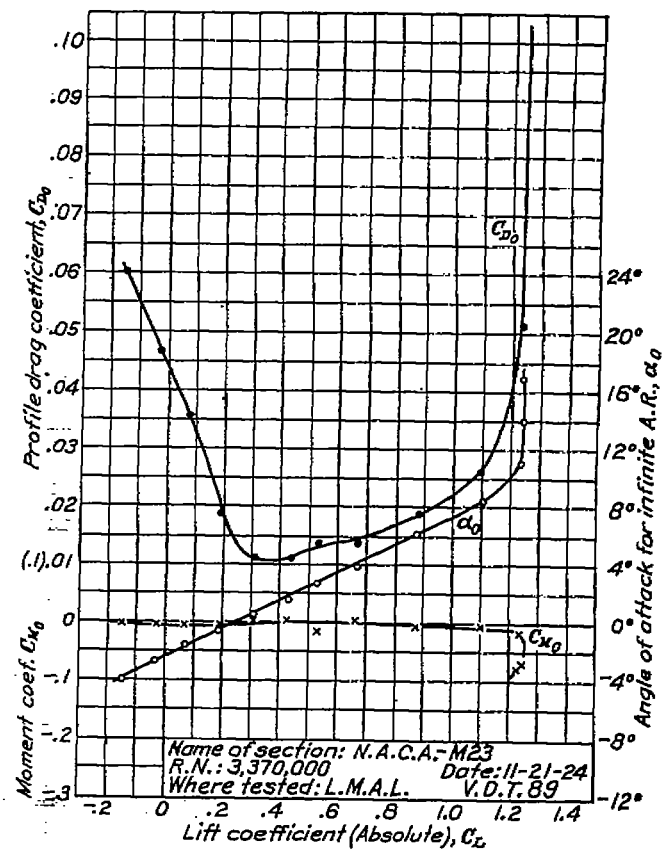

FIGURE 53.—N. A. C. A.-M23 airfoil characteristics corrected to infinite aspect ratio

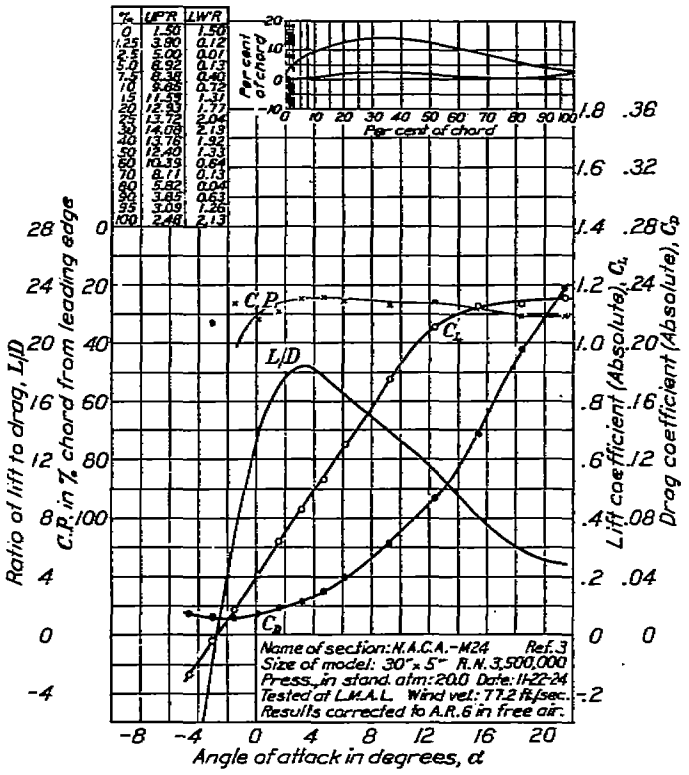

FIGURE 54.—N. A. C. A.-M24 airfoil characteristics corrected to aspect ratio 6

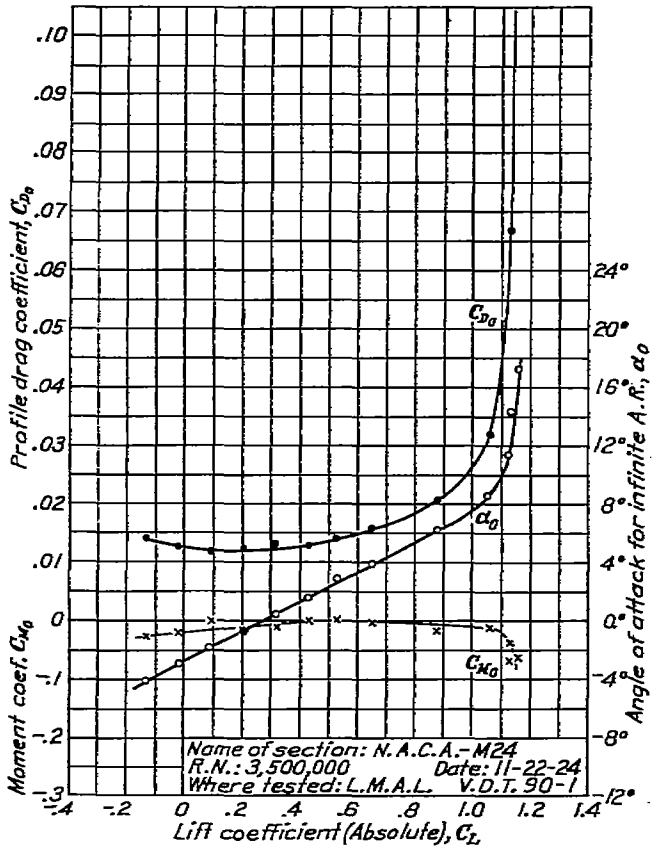

FIGURE 55.—N. A. C. A.-M24 airfoil characteristics corrected to infinite aspect ratio

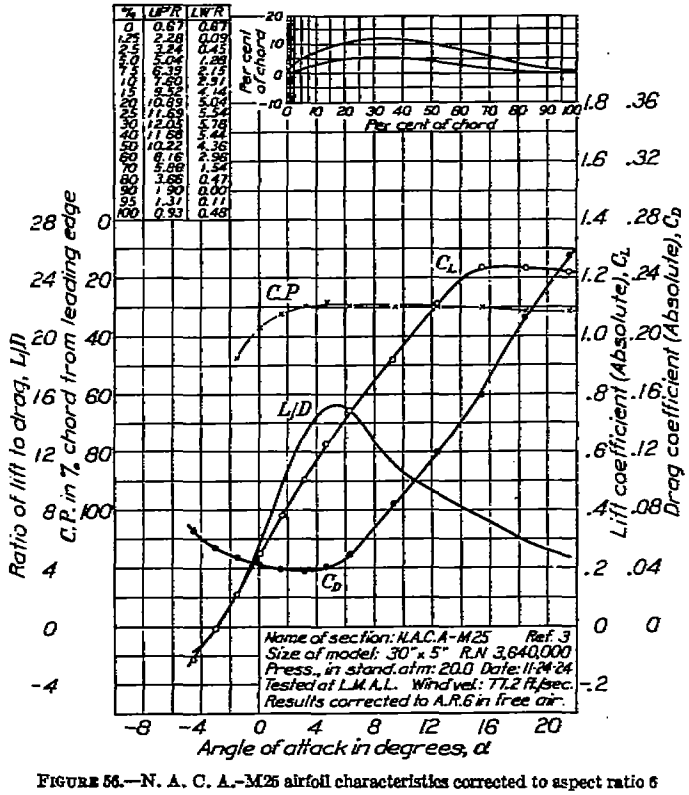

FIGURE 56.—N. A. C. A.-M25 airfoil characteristics corrected to aspect ratio 6

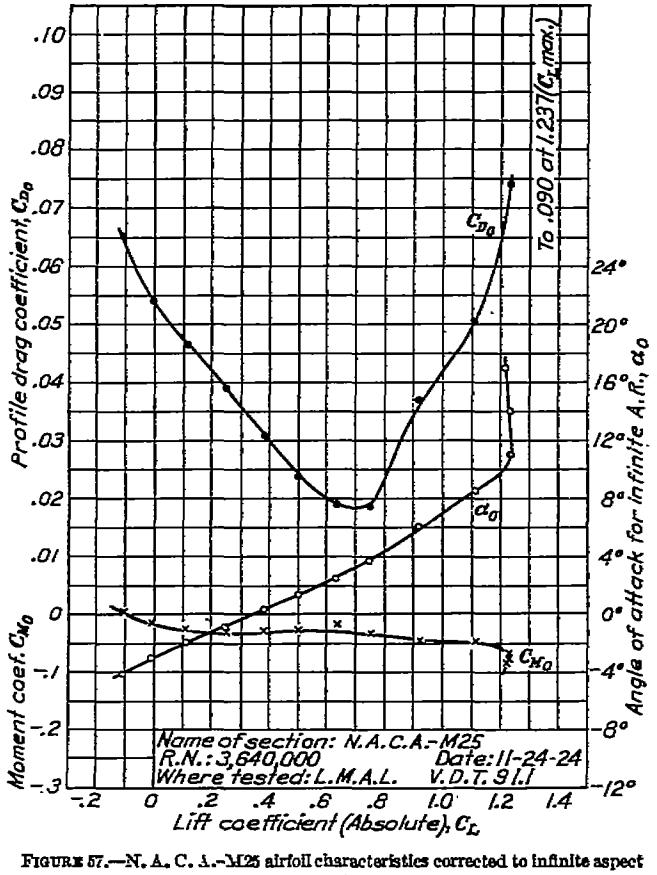

FIGURE 57.—N. A. C. A.-M25 airfoil characteristics corrected to infinite aspect ratio

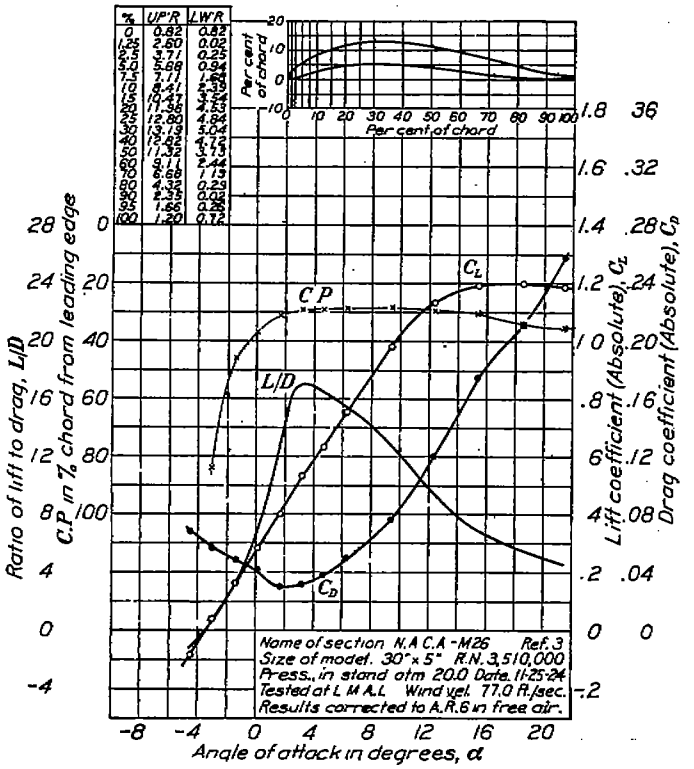

FIGURE 58.—N. A. C. A.-M26 airfoil characteristics corrected to aspect ratio 6

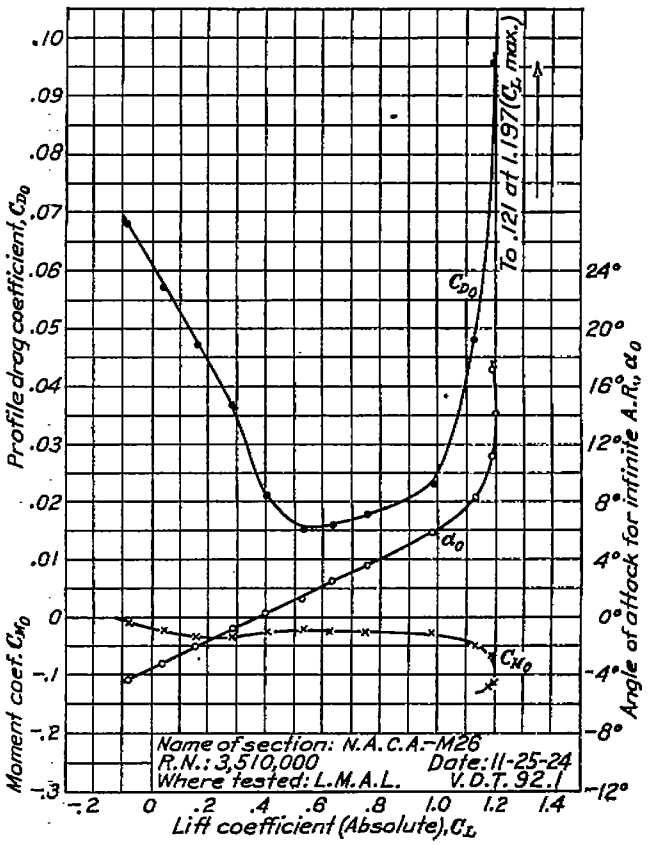

FIGURE 59.—N. A. C. A.-M26 airfoil characteristics corrected to infinite aspect ratio

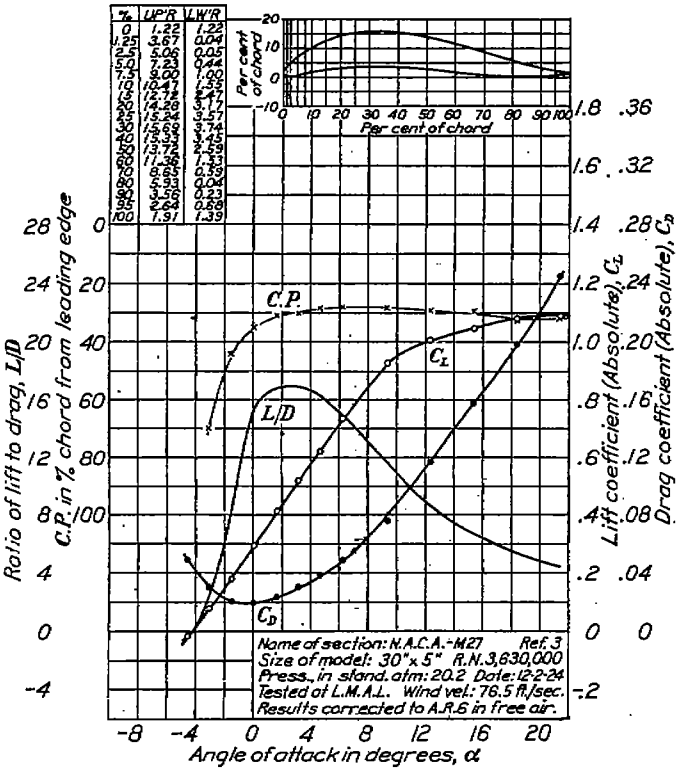

FIGURE 60.—N. A. C. A.-M27 airfoil characteristics corrected to aspect ratio 6

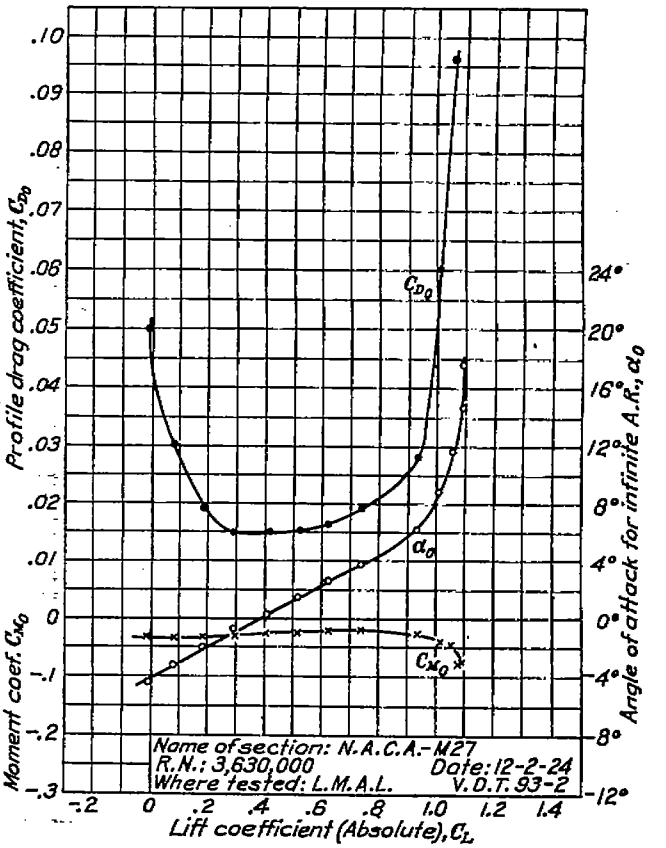

FIGURE 61.—N. A. C. A.-M27 airfoil characteristics corrected to infinite aspect ratio

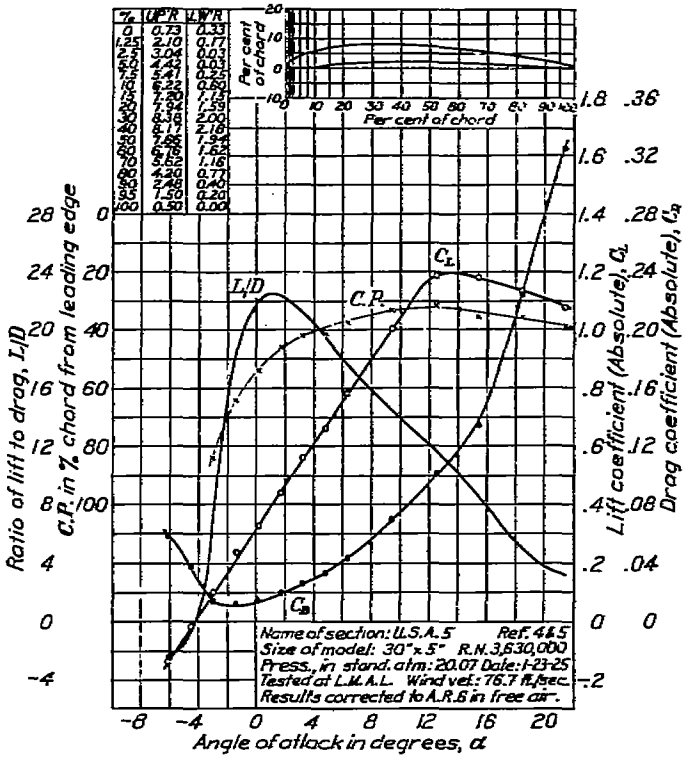

FIGURE 62.—U. S. A. 5 airfoil characteristics corrected to aspect ratio 6

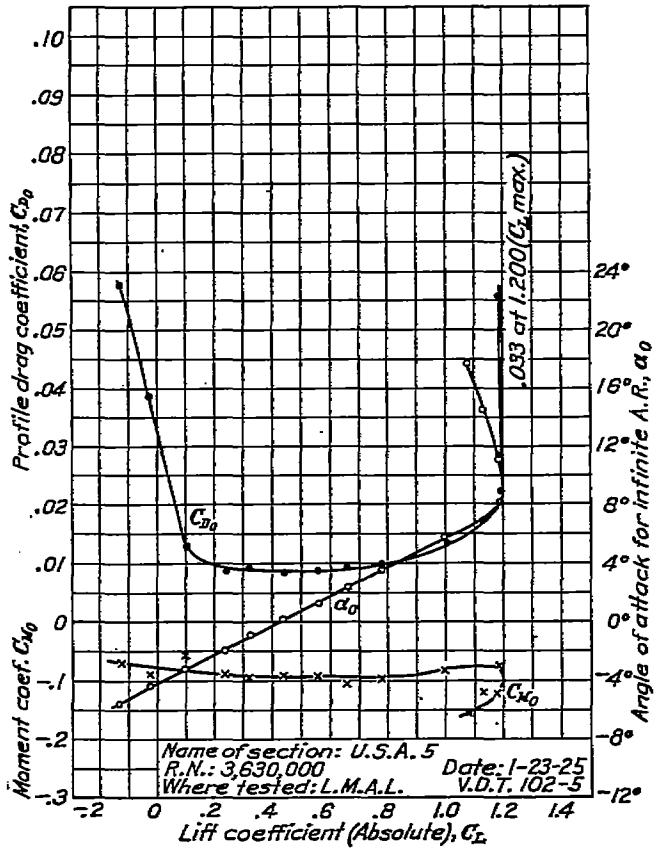

FIGURE 63.—U. S. A. 5 airfoil characteristics corrected to infinite aspect ratio

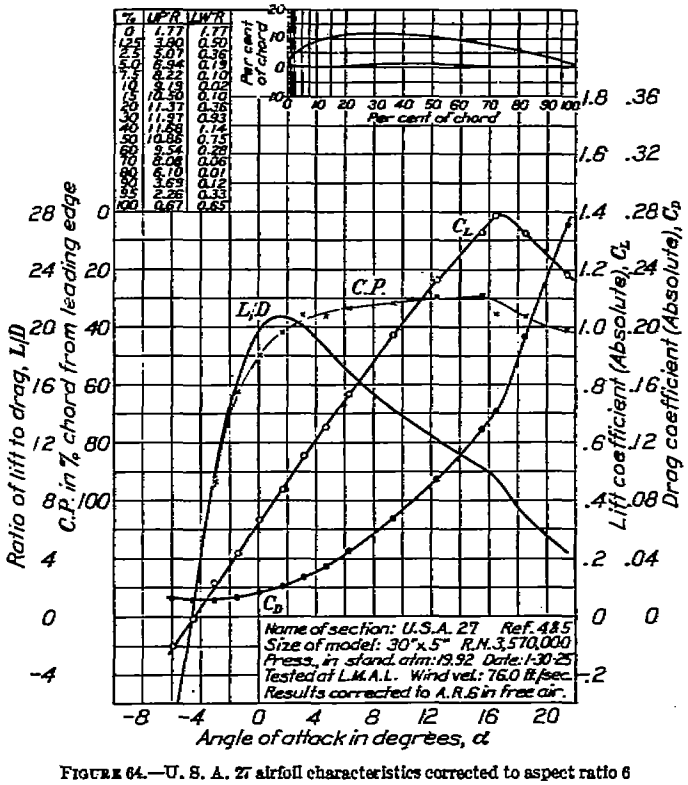

FIGURE 64.—U. S. A. 27 airfoil characteristics corrected to aspect ratio 6

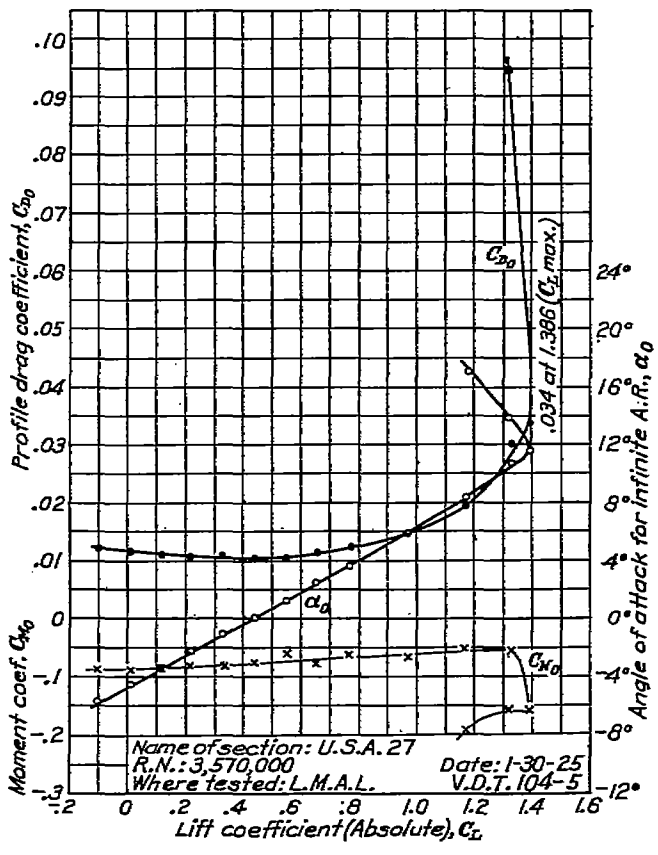

FIGURE 65.—U. S. A. 27 airfoil characteristics corrected to infinite aspect ratio

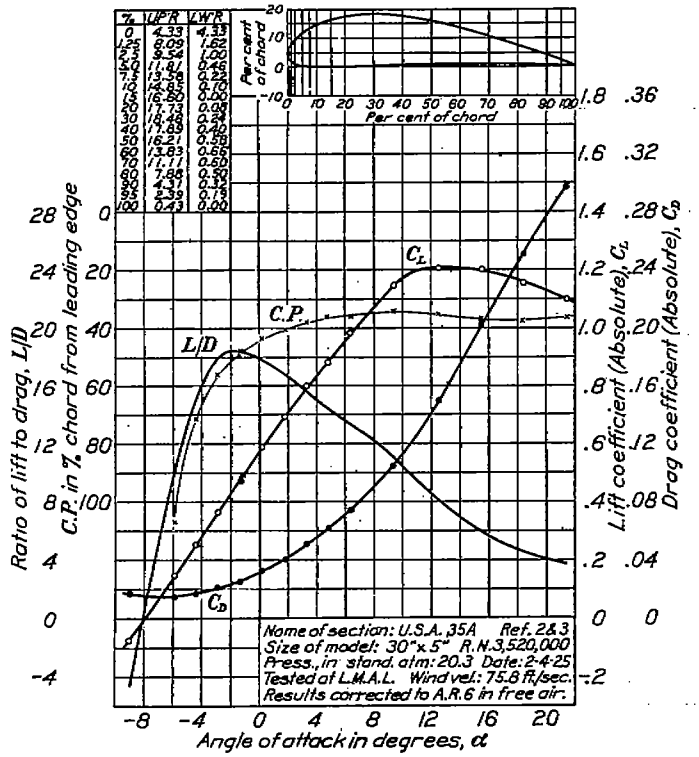

FIGURE 66.—U. S. A. 35A airfoil characteristics corrected to aspect ratio 6

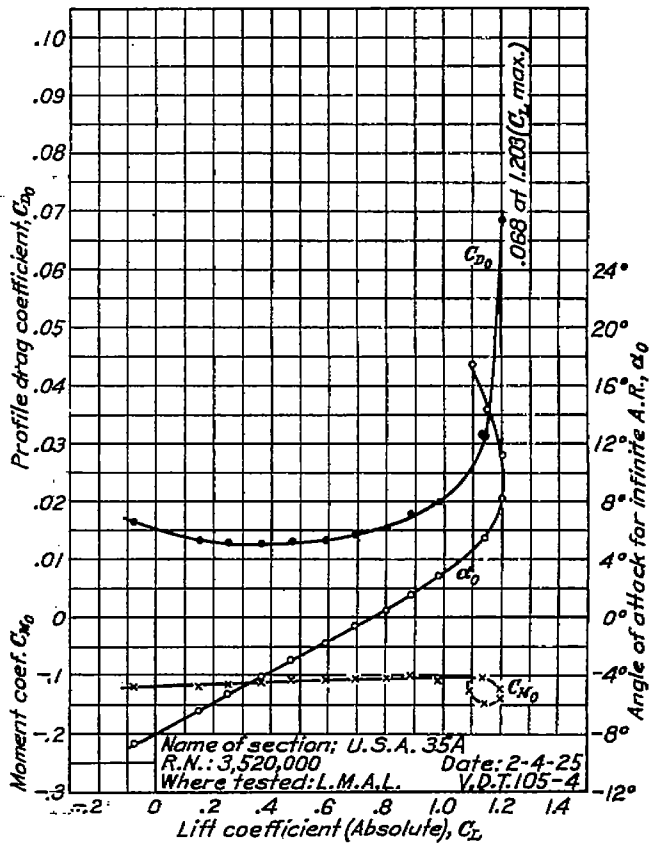

FIGURE 67.—U. S. A. 35A airfoil characteristics corrected to infinite aspect ratio

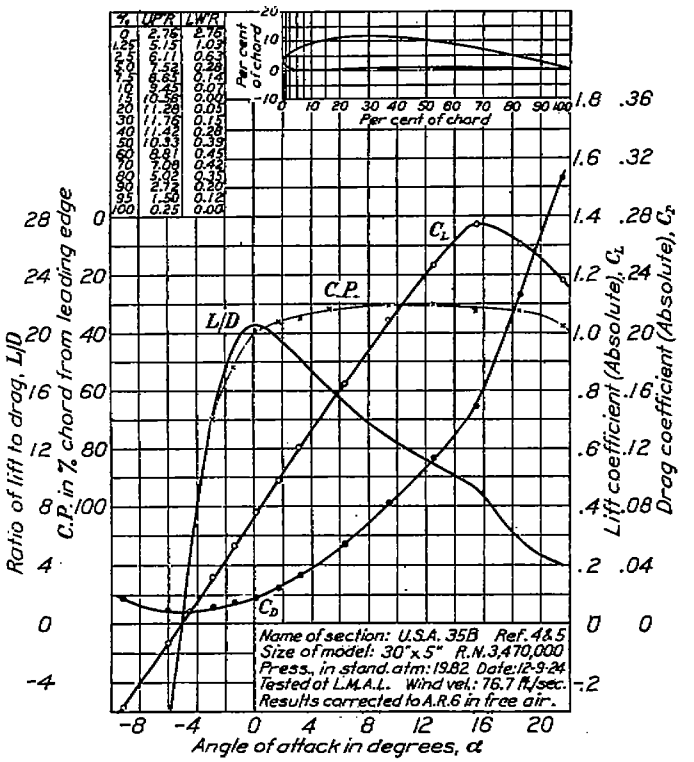

FIGURE 68.—U. S. A. 35B airfoil characteristics corrected to aspect ratio 6

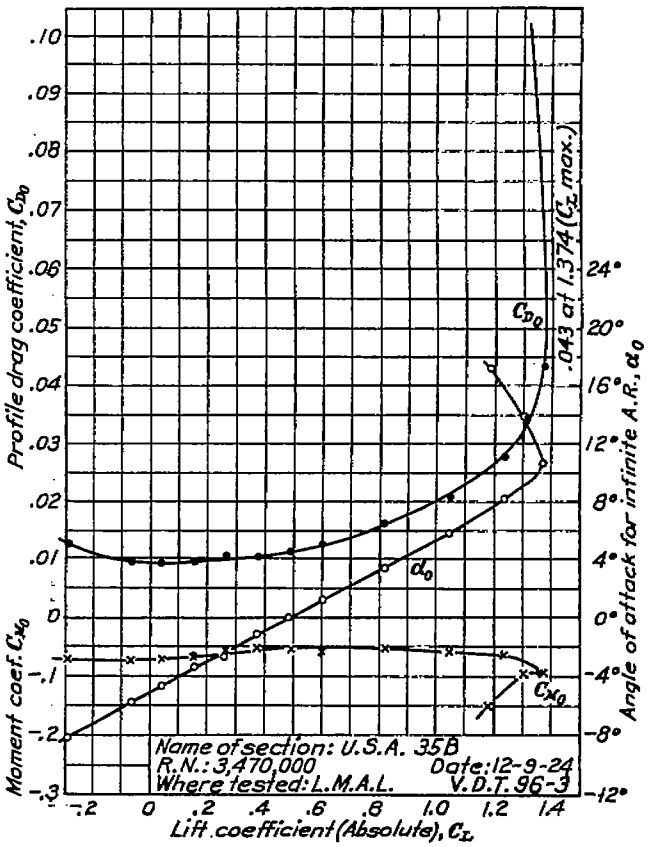

FIGURE 69.—U. S. A. 35B airfoil characteristics corrected to infinite aspect ratio

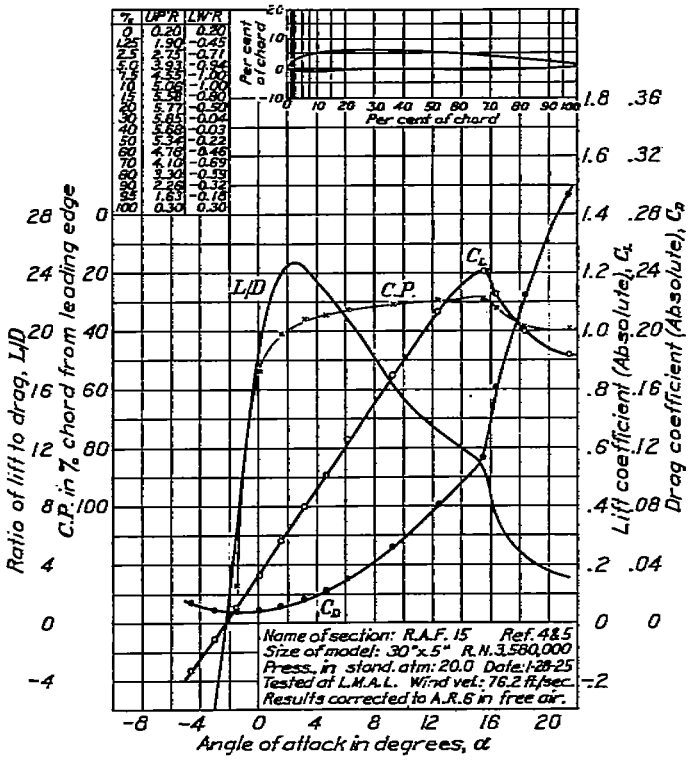

FIGURE 70.—R. A. F. 15 airfoil characteristics corrected to aspect ratio 6

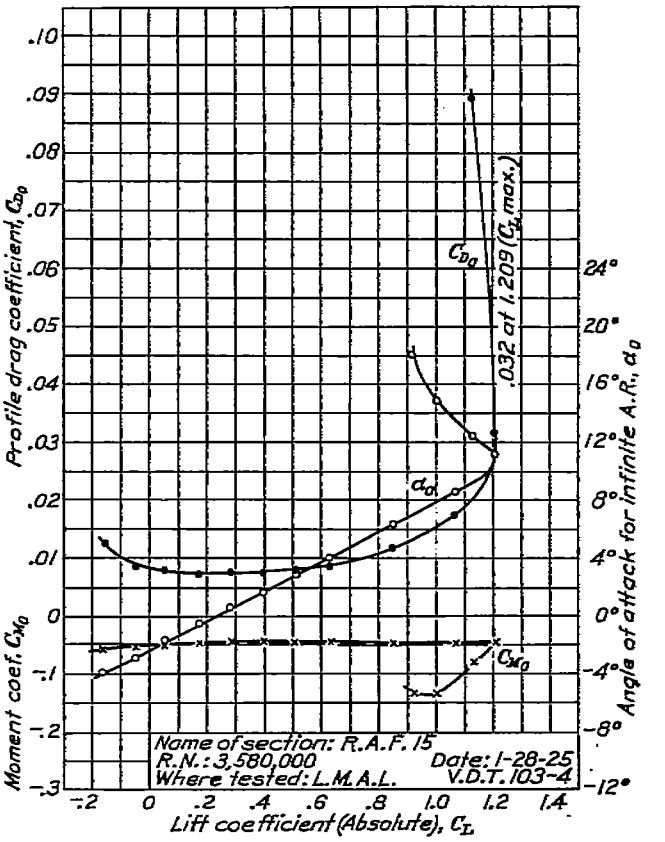

FIGURE 71.—R. A. F. 15 airfoil characteristics corrected to infinite aspect ratio

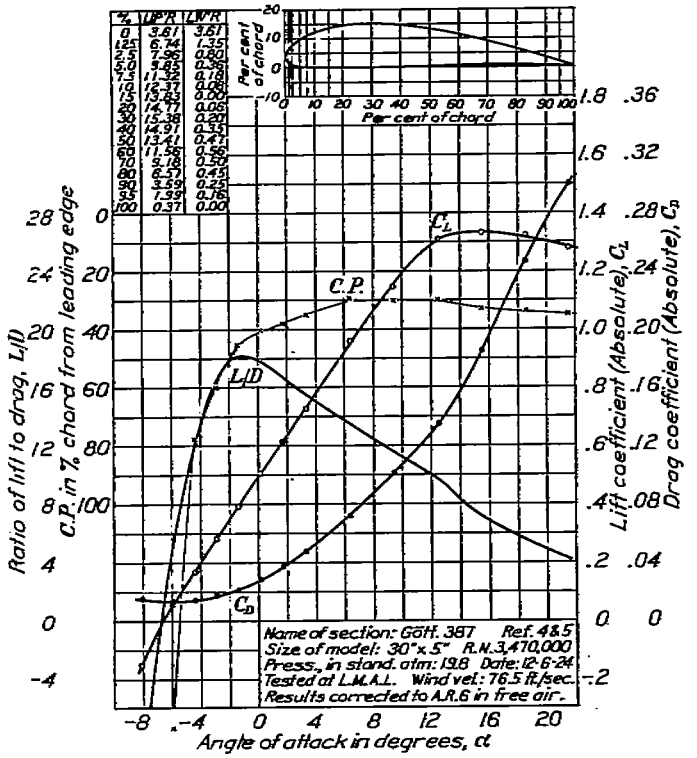

FIGURE 72.—Göttingen 387 airfoil characteristics corrected to aspect ratio 6

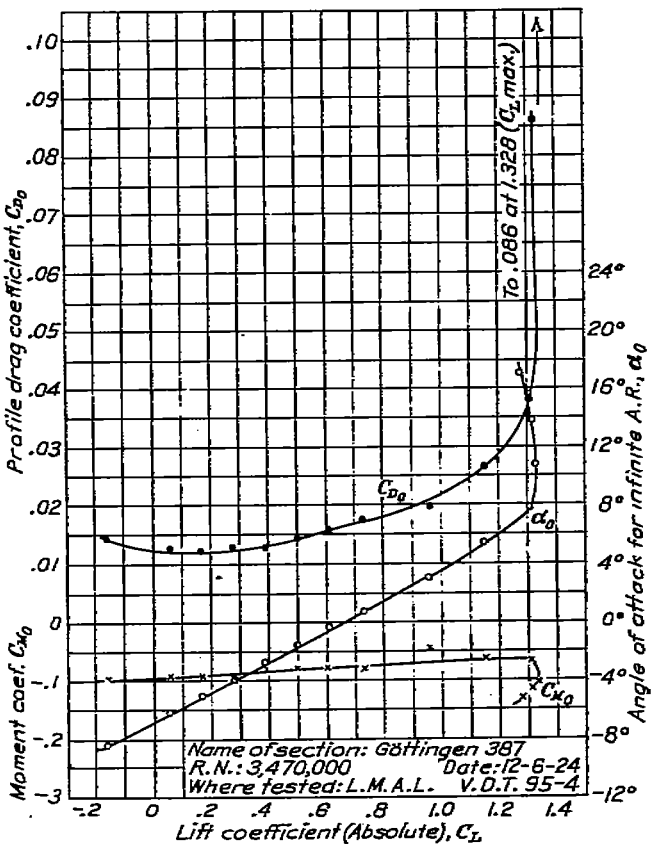

FIGURE 73.—Göttingen 387 airfoil characteristics corrected to infinite aspect ratio

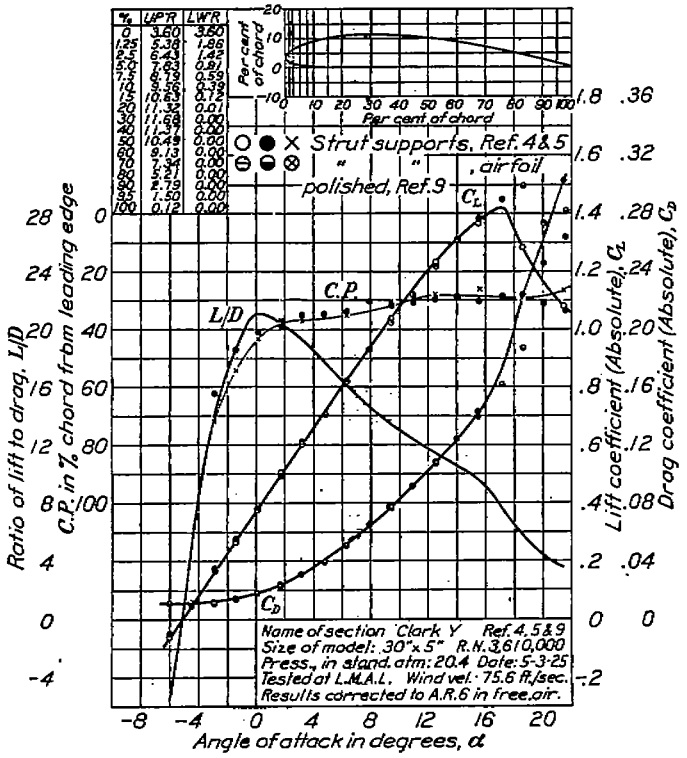

FIGURE 74.—Clark Y airfoil characteristics corrected to aspect ratio 6

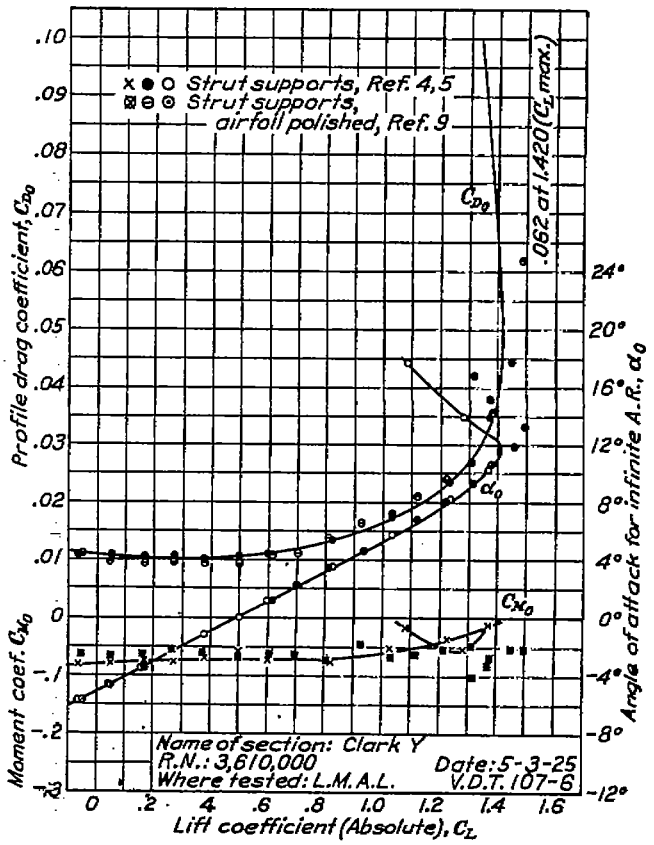

FIGURE 75.—Clark Y airfoil characteristics corrected to infinite aspect ratio

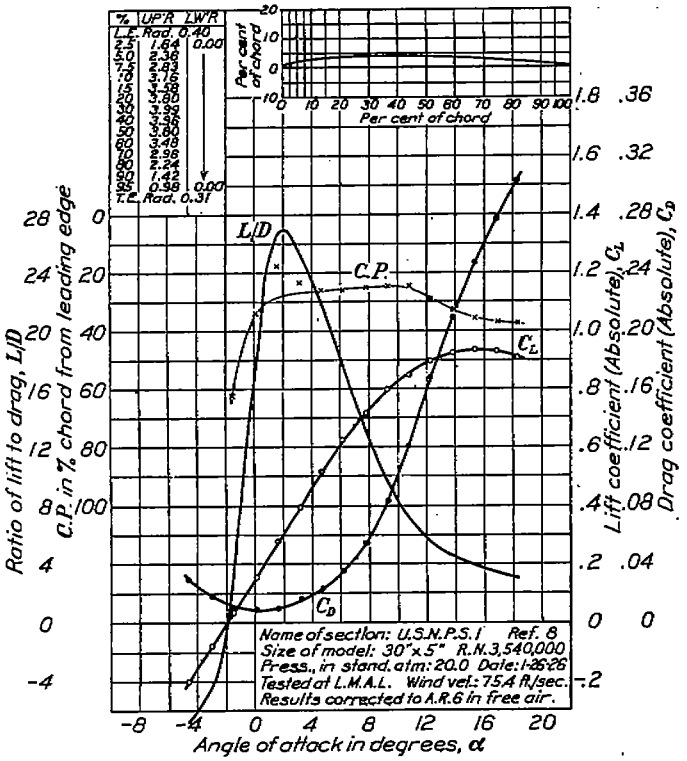

FIGURE 76.—U. S. N. P .S. 1 airfoil characteristics corrected to aspect ratio 6

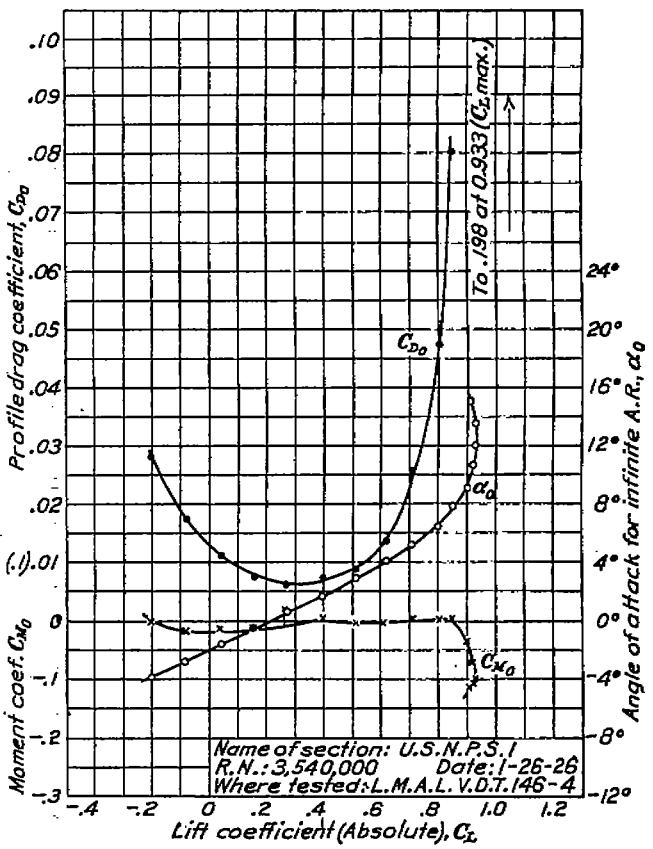

FIGURE 77.—U. S. N. P. S. 1 airfoil characteristics corrected to infinite aspect ratio

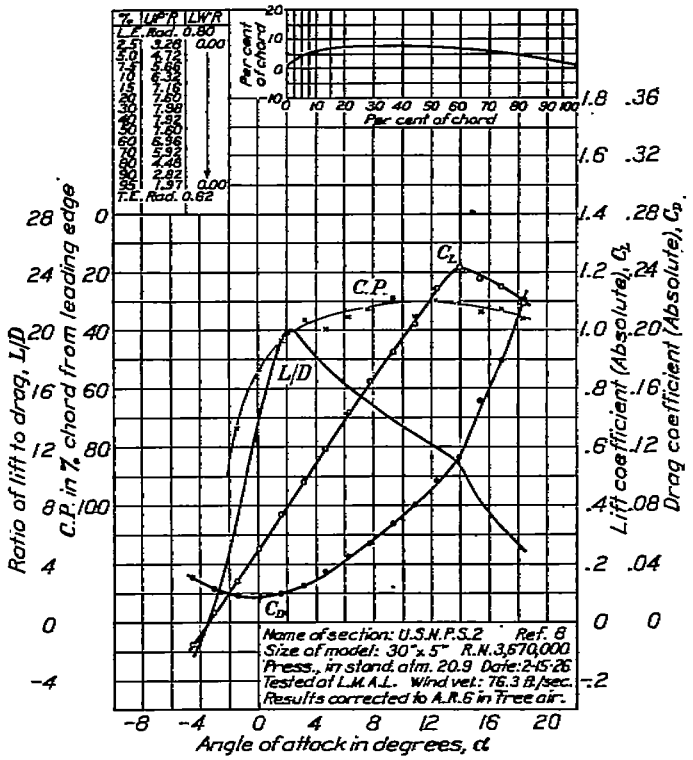

FIGURE 78.—U. S. N. P. S. 2 airfoil characteristics corrected to aspect ratio 6

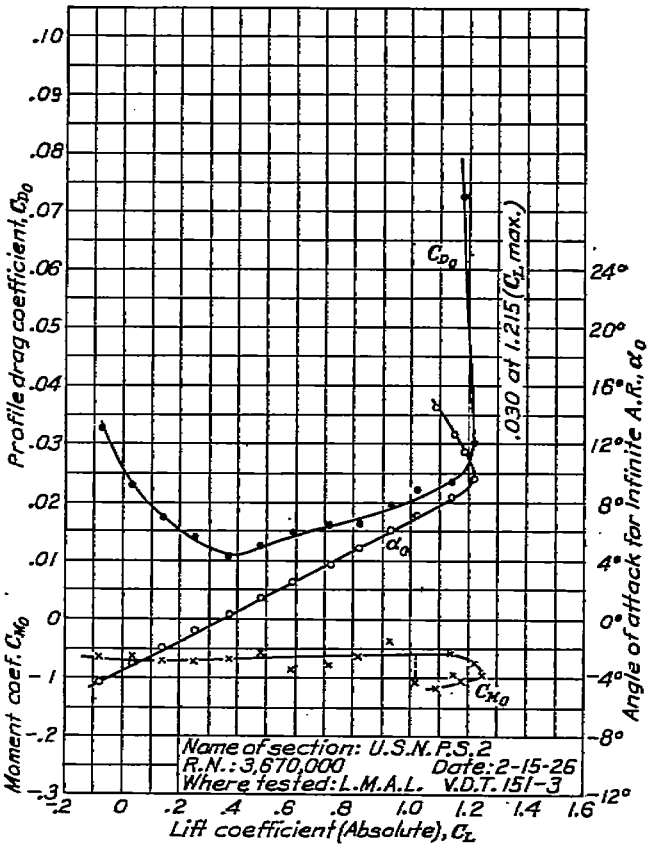

FIGURE 79.—U. S. N. P. S. 2 airfoil characteristics corrected to infinite aspect ratio

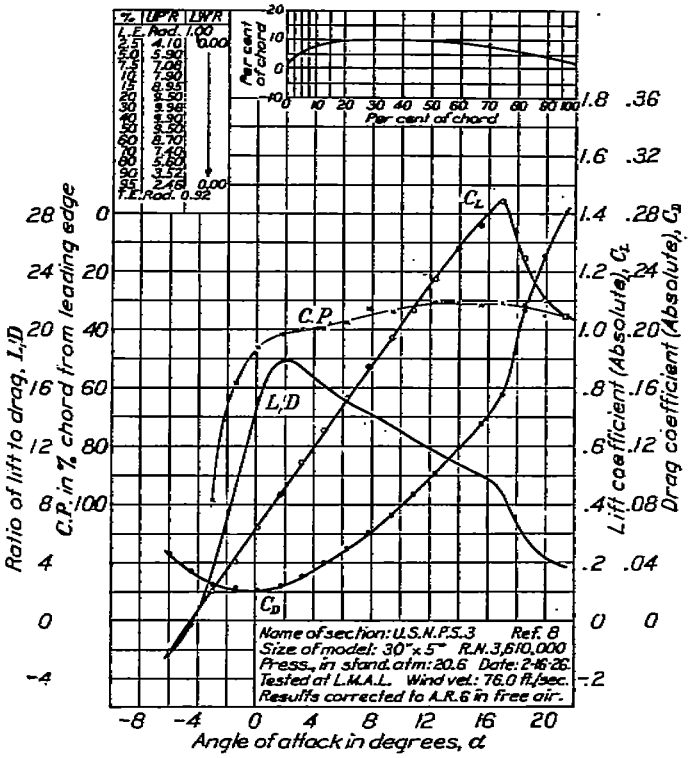

FIGURE 80.—U. S. N. P. S. 3 airfoil characteristics corrected to aspect ratio 6

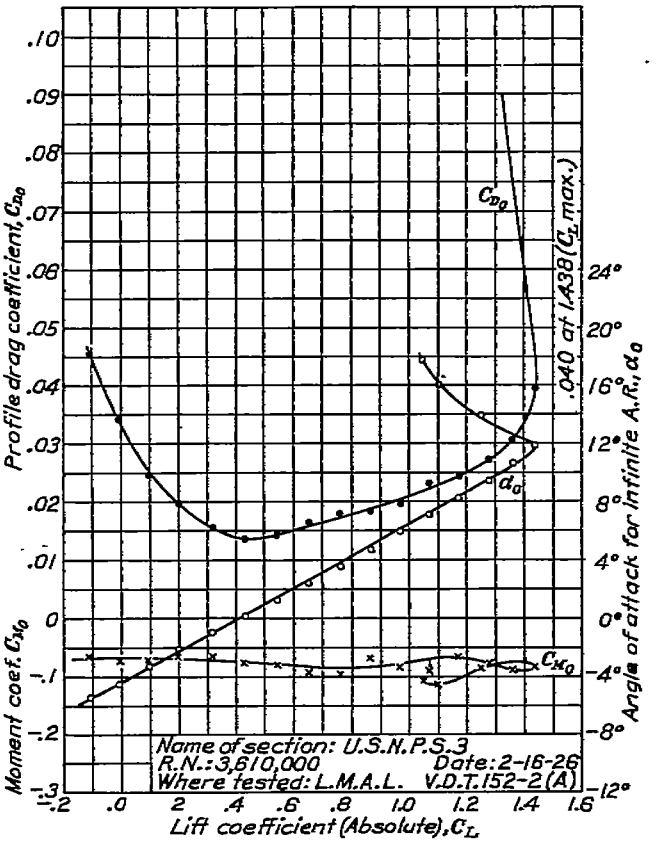

FIGURE 81.—U. S. N. P. S. 3 airfoil characteristics corrected to infinite aspect ratio

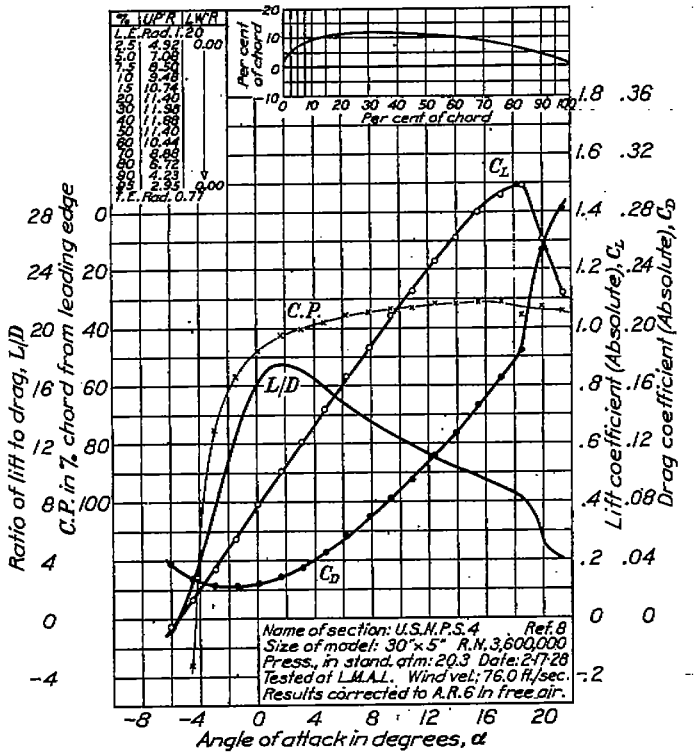

FIGURE 82.—U. S. N. P. S. 4 airfoil characteristics corrected to aspect ratio 6

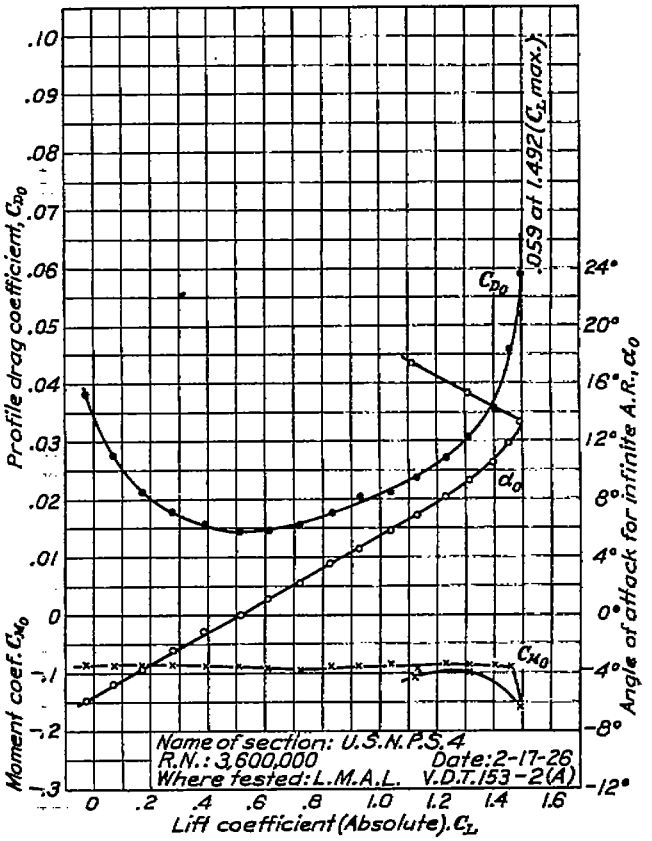

FIGURE 83.—U. S. N. P. S. 4 airfoil characteristics corrected to infinite aspect ratio

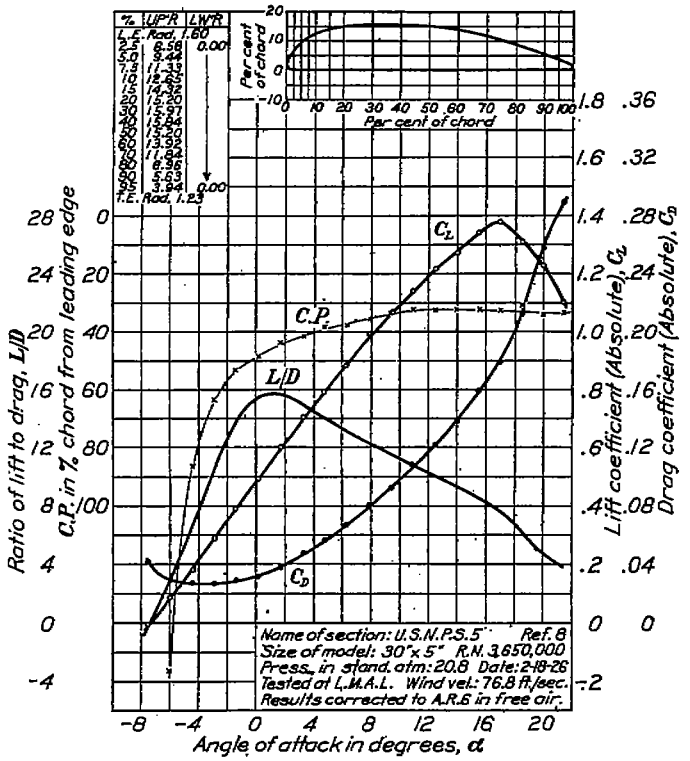

FIGURE 84.—U. S. N. P. S. 5 airfoil characteristics corrected to aspect ratio 6

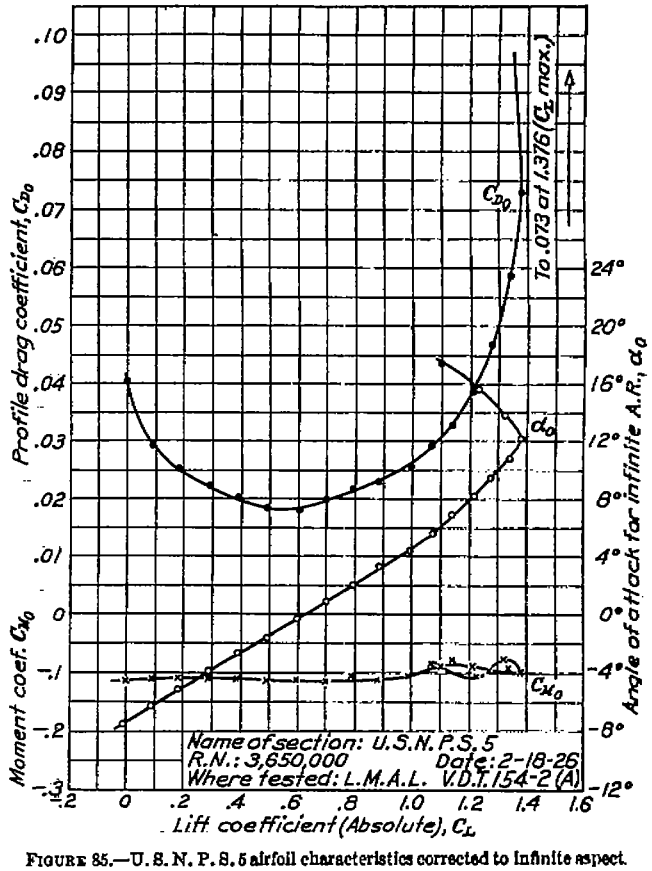

FIGURE 85.—U. S. N. P. S. 5 airfoil characteristics corrected to infinite aspect ratio

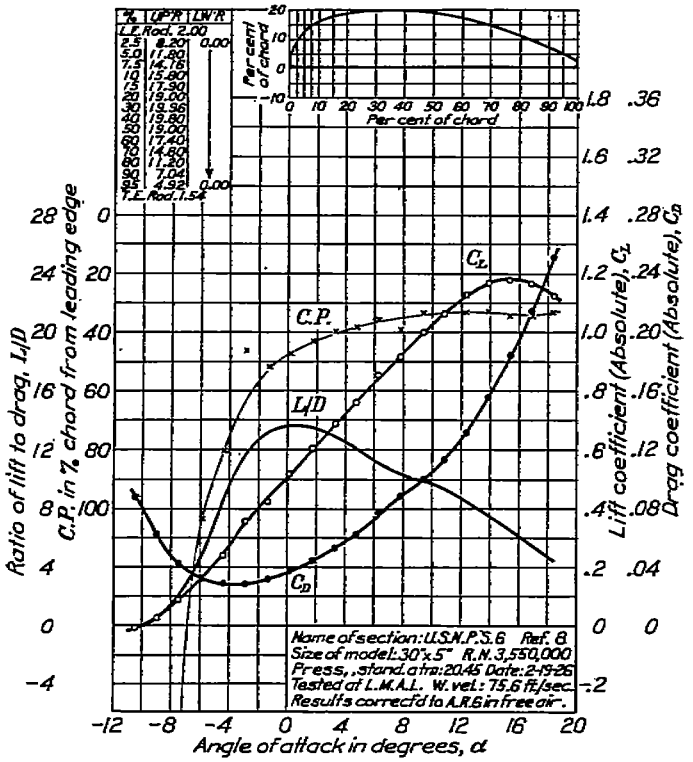

FIGURE 86.—U. S. N. P. S. 6 airfoil characteristics corrected to aspect ratio 6

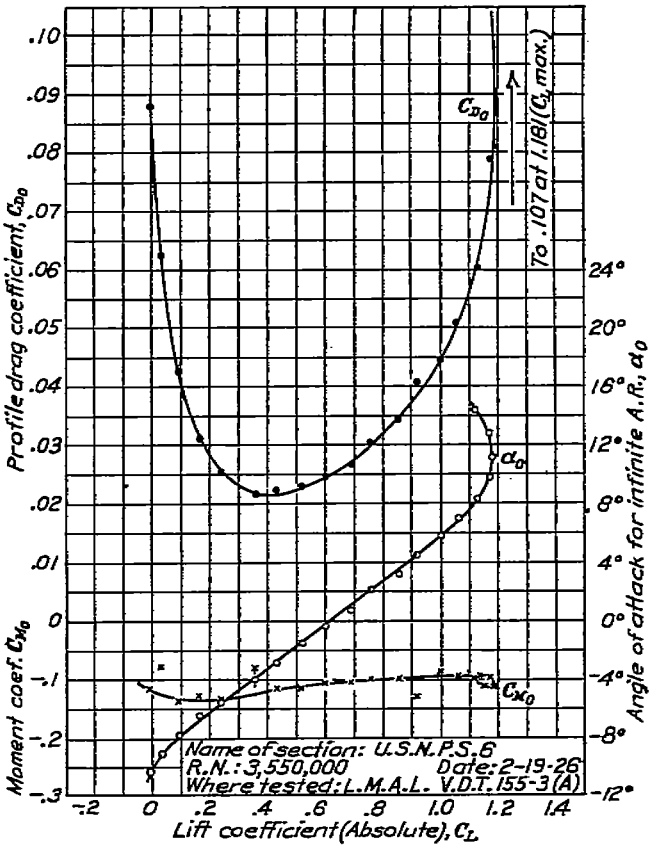

FIGURE 87.—U. S. N. P. S. 6 airfoil characteristics corrected to infinite aspect ratio

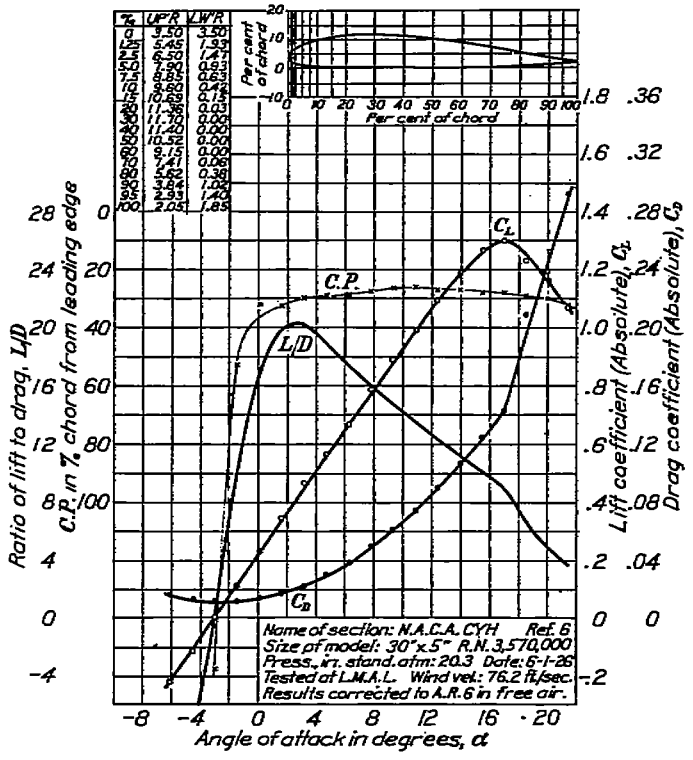

FIGURE 88.—N. A. C. A. CYH airfoil characteristics corrected to aspect ratio 6

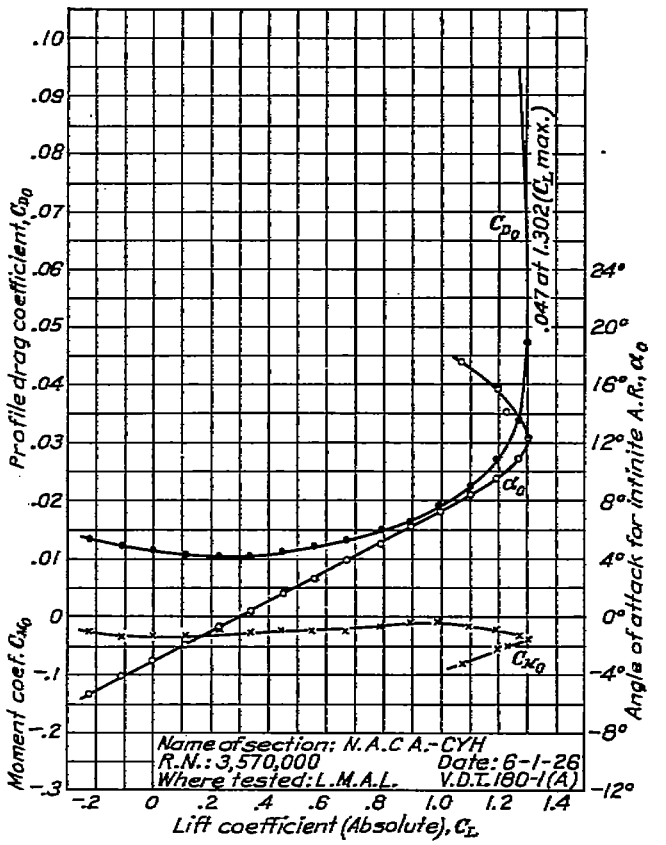

FIGURE 89.—N. A. C. A. CYH airfoil characteristics corrected to infinite aspect ratio

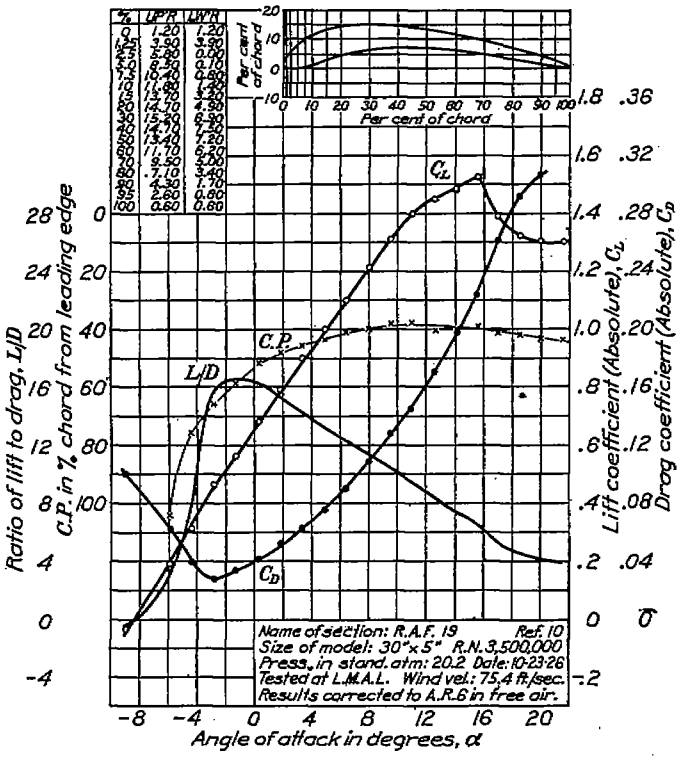

FIGURE 90.—R. A. F. 19 airfoil characteristics corrected to aspect ratio 6

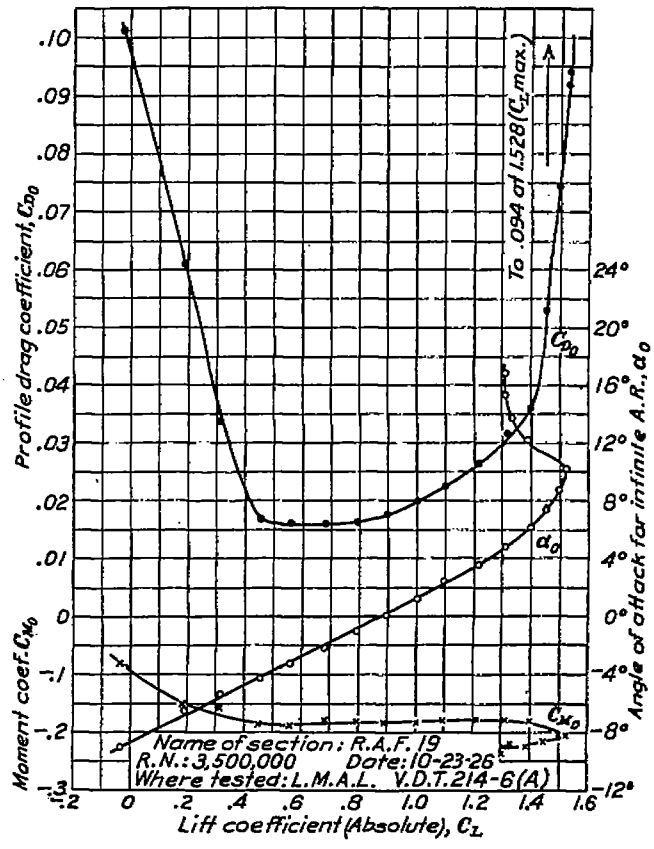

FIGURE 91.—R. A. F. 19 airfoil characteristics corrected to infinite aspect ratio

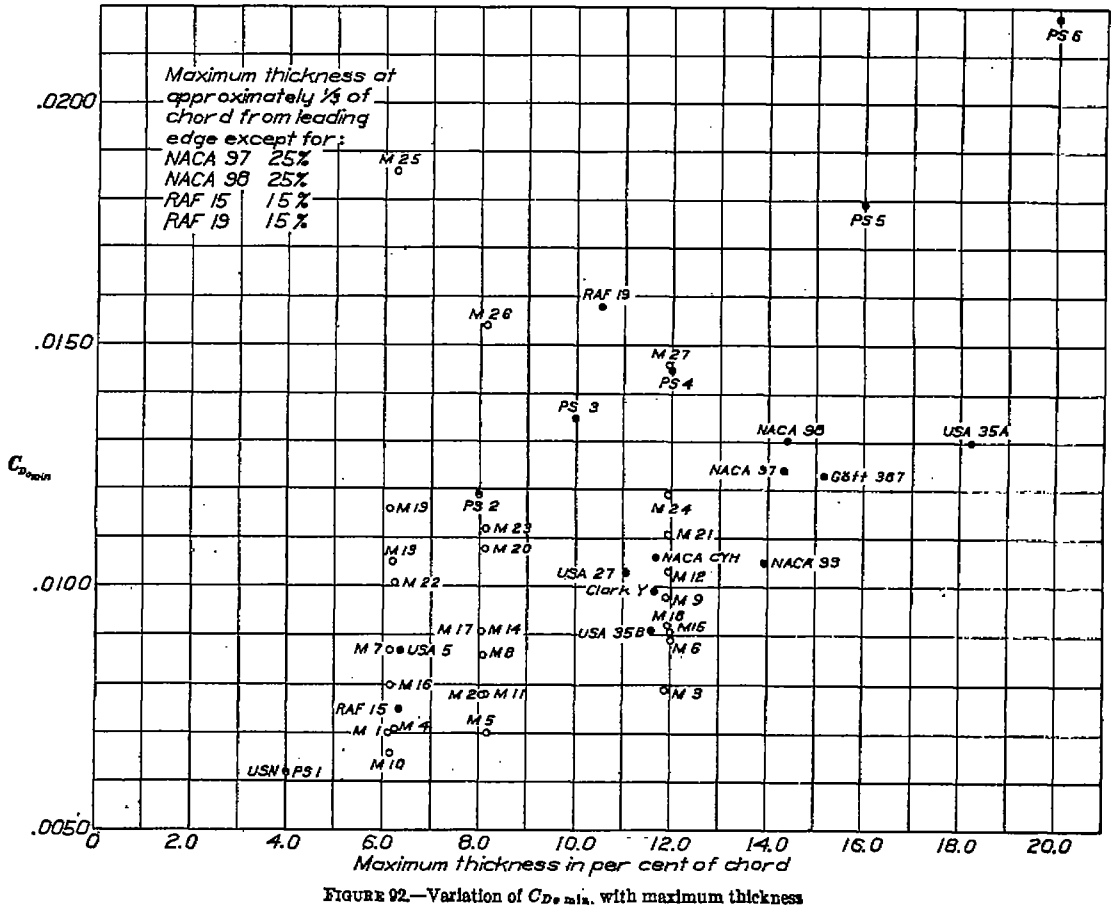

FIGURE 92.—Variation of $C_{D_{min.}}$ with maximum thickness

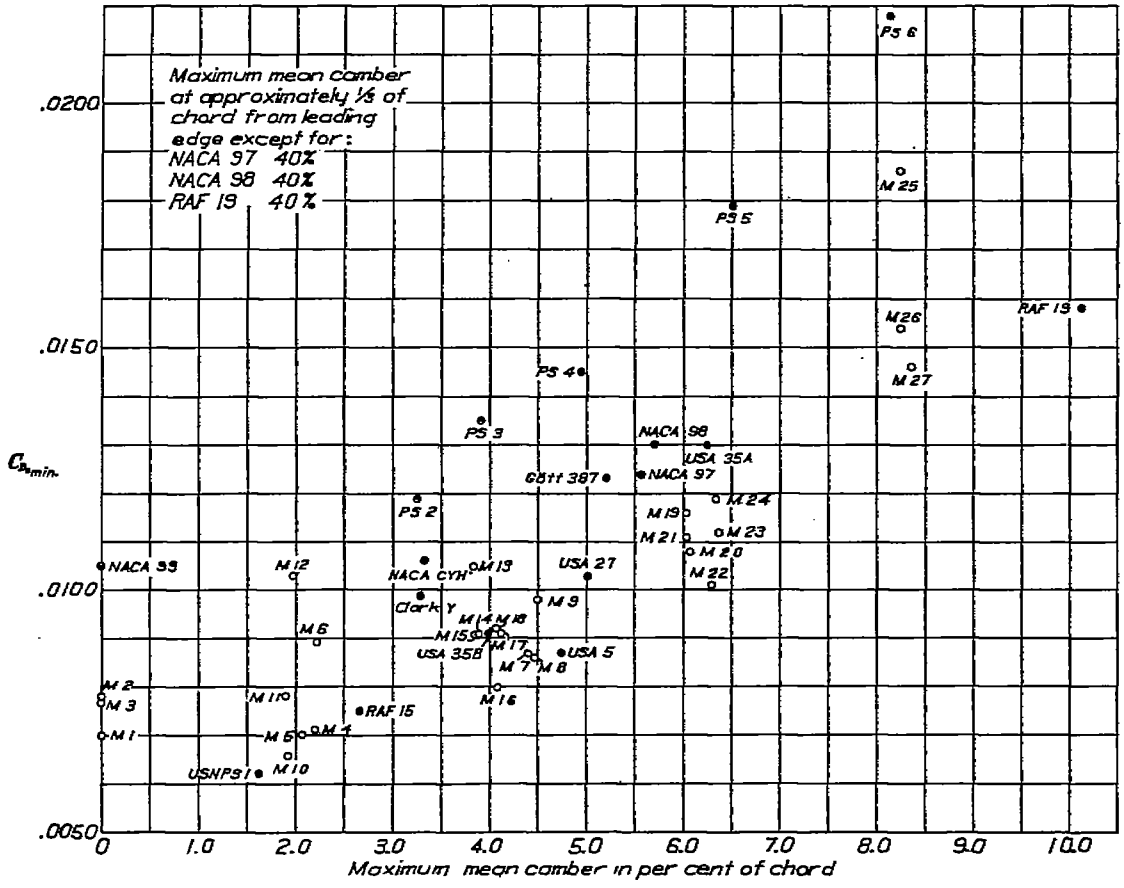

FIGURE 93.—Variation of $C_{D_{min.}}$ with maximum mean camber

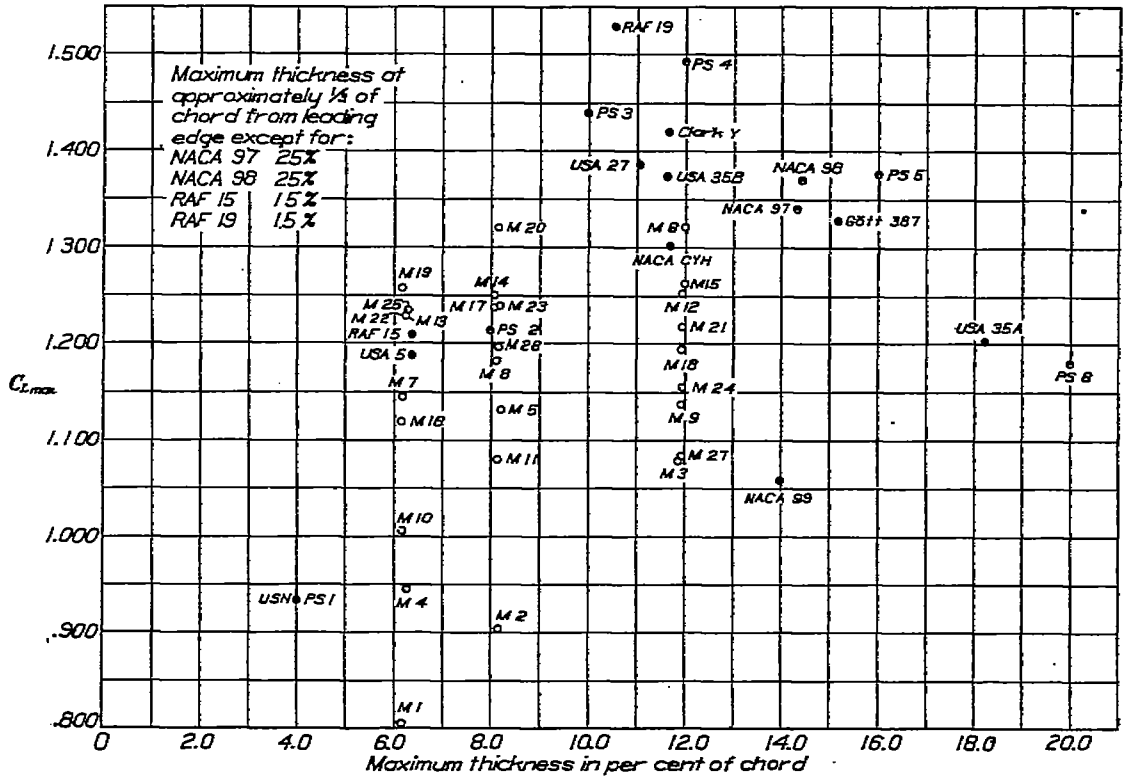

FIGURE 94.—Variation of with $C_{L_{max.}}$ with maximum thickness

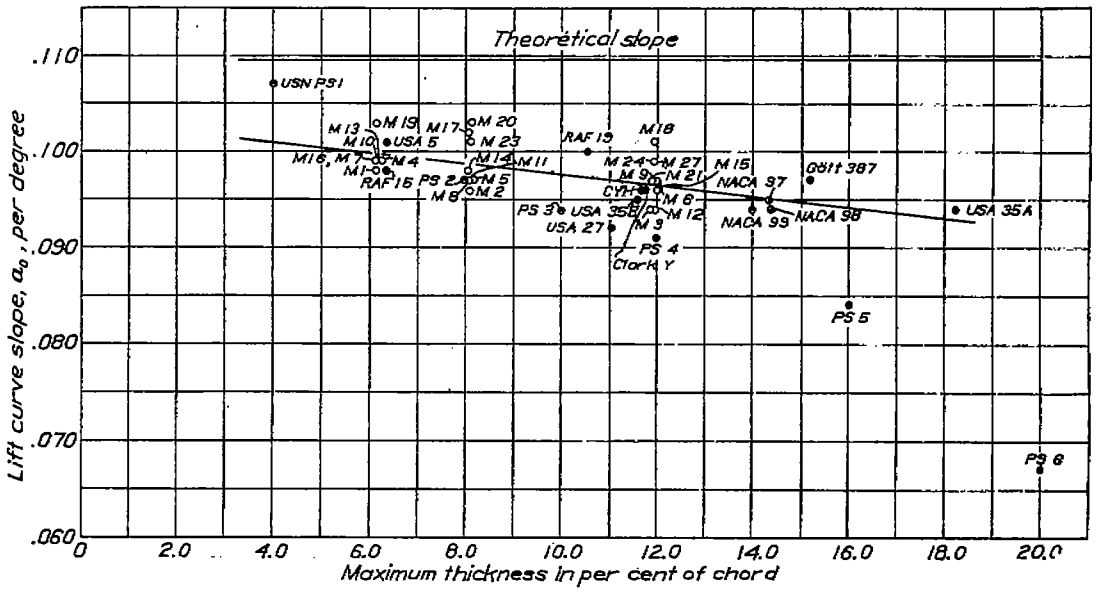

FIGURE 95.—Variation with maximum thickness of lift curve slope for wings of infinite aspect ratio

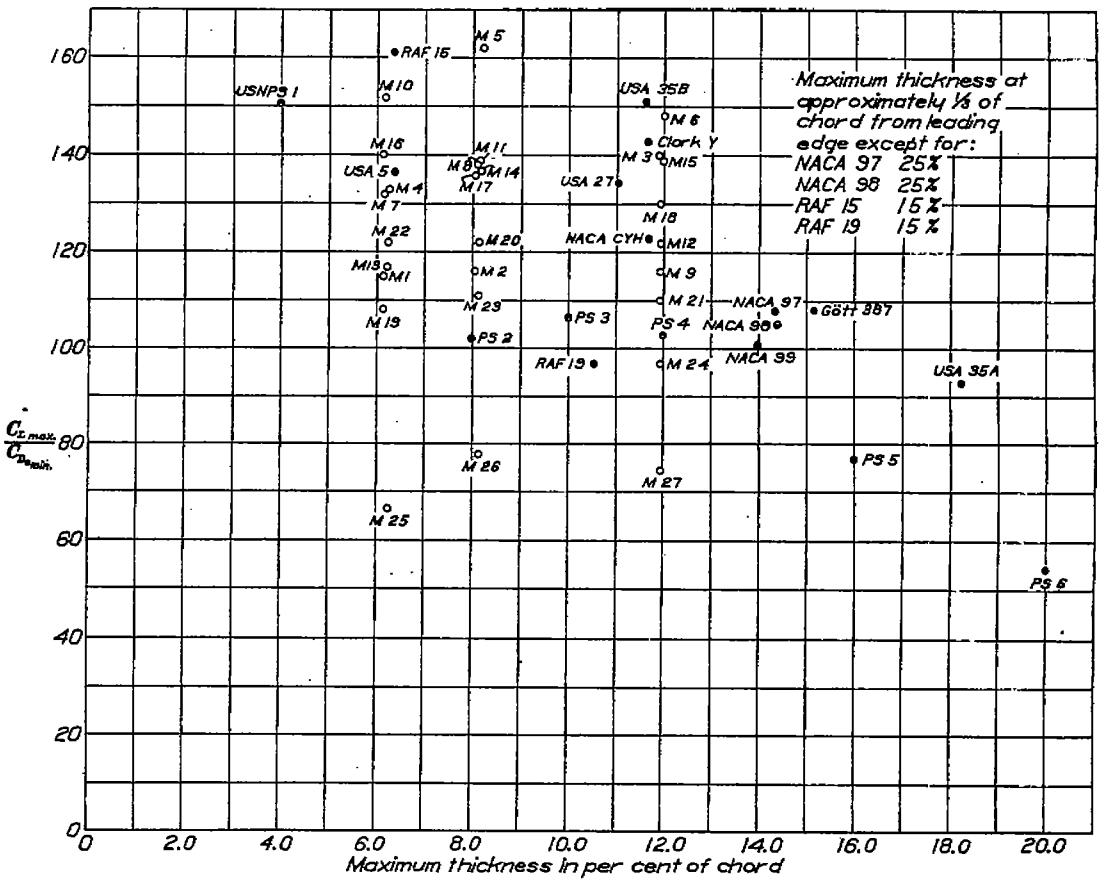

FIGURE 96.—Variation of $\frac{C_{L\,max.}}{C_{D_0\,min.}}$ with maximum thickness